1999

Petrogenesis of the Adel Mountains volcanic field central Montana

Betsy Cunningham
The University of Montana

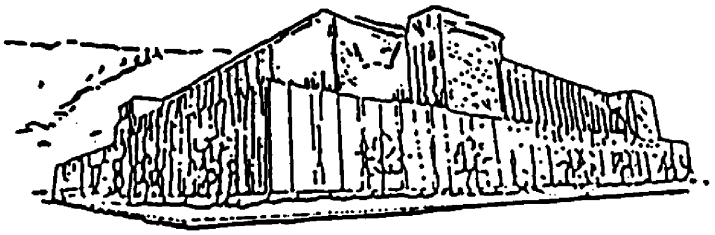

Maureen and Mike
MANSFIELD LIBRARY

The University of **MONTANA**

** *Please check "Yes" or "No" and provide signature* **

Yes, I grant permission X
No, I do not grant permission ____

Author's Signature Betsey L. Angle

Date May 10, 1999

PETROGENESIS OF THE ADEL MOUNTAINS VOLCANIC FIELD, CENTRAL MONTANA

by
Betsy Cunningham
B.A. Colgate University 1997

presented in partial fulfillment of the requirements
for the degree of Master of Science
The University of Montana
1999

Approved by:

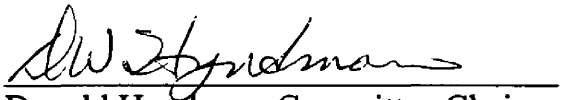

Donald Hyndman, Committee Chair

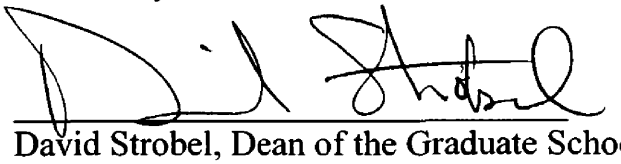

David Strobel, Dean of the Graduate School

5-17-99

Date

ProQuest LLC.
789 East Eisenhower Parkway
P.O. Box 1346
Ann Arbor, MI 48106 - 1346

Cunningham, Betsy L., M.S., May 1999 Geology

PETROGENESIS OF THE ADEL MOUNTAINS, CENTRAL MONTANA (82 pp.)

Director: Donald Hyndman

The Adel Mountains volcanic pile within the central Montana Alkalic Province (also referred to as the high potassium province) has been $^{40}Ar/^{39}Ar$ dated at 73.6 ± 0.7 Ma with a 1-3 My period of igneous activity (Harlan 1991). Shonkinite, a high potassium, salite-bearing rock, is volumetrically dominant in the Adels although latite, alkalic basalt, and syenite are also present in decreasing proportions, respectively. A genetic relationship between shonkinite and syenite observed both in field and chemical data, which strongly suggests immiscible liquid separation is responsible for the formation of syenite. Evidence for immiscible separation includes the presence of syenite veinlets and globules, and enriched titanium, phosphorous, cesium, and lanthanum concentrations in the mafic host.

Latite in the volcanic pile was generated by a combination of fractional crystallization and magma mixing from an alkali basalt parent as is evidenced by: a) mixing and fractionation modeling, b) enrichment of latite in Ba, Rb, Zr, Nb, c) extensive zoning in augite grains, and d) co-genetic REE patterns.

Throughout the magmatic history of the Adels, shonkinite was either erupted or intruded in several generations to form dikes which radiate from the Three Sisters Stock and are described in detail by Beall (1973) and Hyndman and Alt (1987). In the present study, some dikes are found to mingle with earlier erupted shonkinite flows or with intrusive basaltic dikes forming co-mingling features. This suggests that both shonkinite and alkalic basalt must have been magmatic at the same time in the same place.

Modeling an environment where basalt and shonkinite are generated simultaneously in time and space is complex. The Wyoming craton is inferred to truncate near the southwestern edge of the Adel Mountains. A sloping cratonic boundary could be mimicked in the mantle. Partial melting of the mantle beneath the Wyoming craton would produce basalt. However, due to the sloping geometry of such a feature, anomalously alkalic mantle beneath central Montana would also be present. Partial melting of this high potassium mantle would result in shonkinite melts. Partial melting of the overlapping boundaries between the two mantle compositions is compatible with generating contemporaneous shonkinite and basalt. This model is supported by increasing potassium contents in the Bearpaw Mountains north of the Adels, and a mixture of both high potassium and basaltic melts to the south in the Elkhorn Mountains.

ACKNOWLEDGEMENTS

As in any geologic study, this project would not have been possible without the knowledge and assistance of many exceptional individuals. I would first like to thank Dr. Don Hyndman, my advisor in every sense of the word, for his patience throughout my graduate career and for helping me to understand the virtues of research, running, and red wine. I would also like to thank my other two committee members, Dr. David Alt and Dr. George McRae. A sincere thanks to my trusted field partner Emilie Reagan (now Henry) for gentleness and laughter as well as my esteemed colleagues, Carl, Steen, and Tom for their assistance both in the field and in the lab. Thanks to Robert Luedke, Jim Whitney, Paul Barton, Phil Bethke, and Carter Hearn for many useful comments and discussions. Above all, I would like to thank my family; Mom, Dad, Wendy, and Justin for their perseverance and insight both academically and in life. Mom and Dad have encouraged me to work hard and play hard in life and my sister Wendy has been an admirable example of success in both. And finally, to my fiance William for his trust and support. Funding for this project was provided by GSA, shared grant funds from Dr. Don Hyndman, the University of Montana.

TABLE OF CONTENTS

LIST OF FIGURES page

LIST OF PHOTOGRAPHS page

Chapter 1-1

INTRODUCTION

Many of the complexities regarding the petrogenesis of the Adel Mountains volcanic field have yet to be described as few workers have investigated the volcanic centers along the border of the previously defined alkalic province. Bridging the gap between alkalic rocks to the northeast (Bearpaw Mountains and Highwood Mountains) with rocks previously considered non-alkalic, immediately to the southwest (Elkhorn Mountains), the Adel Mountains are well located for investigation of the relationship between these two distinct volcanic regions (see Figure 1). Our knowledge of relationships in these regions is also lacking. This study attempts to unravel the history of volcanic rocks with proximity to the central Montana Alkalic Province and adjacent to the defined region.

Four primary rock types are present in this 73 Ma Adel Mountains volcanic center; 1) alkalic basalt, 2) shonkinite, 3) monzonite/latite, and 4) syenite, although diversity among the suite is prolific. The relationships between basalt and latite are compatible with partial melting of mid-crustal rocks to form end member latite and a combination of magma mixing and fractional crystallization from alkalic to form intermediate latitic compositions. Syenite formed from immiscible liquid separation from shonkinite. Mingling relationships are apparent in field and petrographic study between generations of shonkinite, basalt and shonkinite, and possibly shonkinite and latite.

Shonkinite and basalt are not co-genetic, so how is it possible for such a diverse magmatic suite to coexist contemporaneously? A tentative model suggests that a

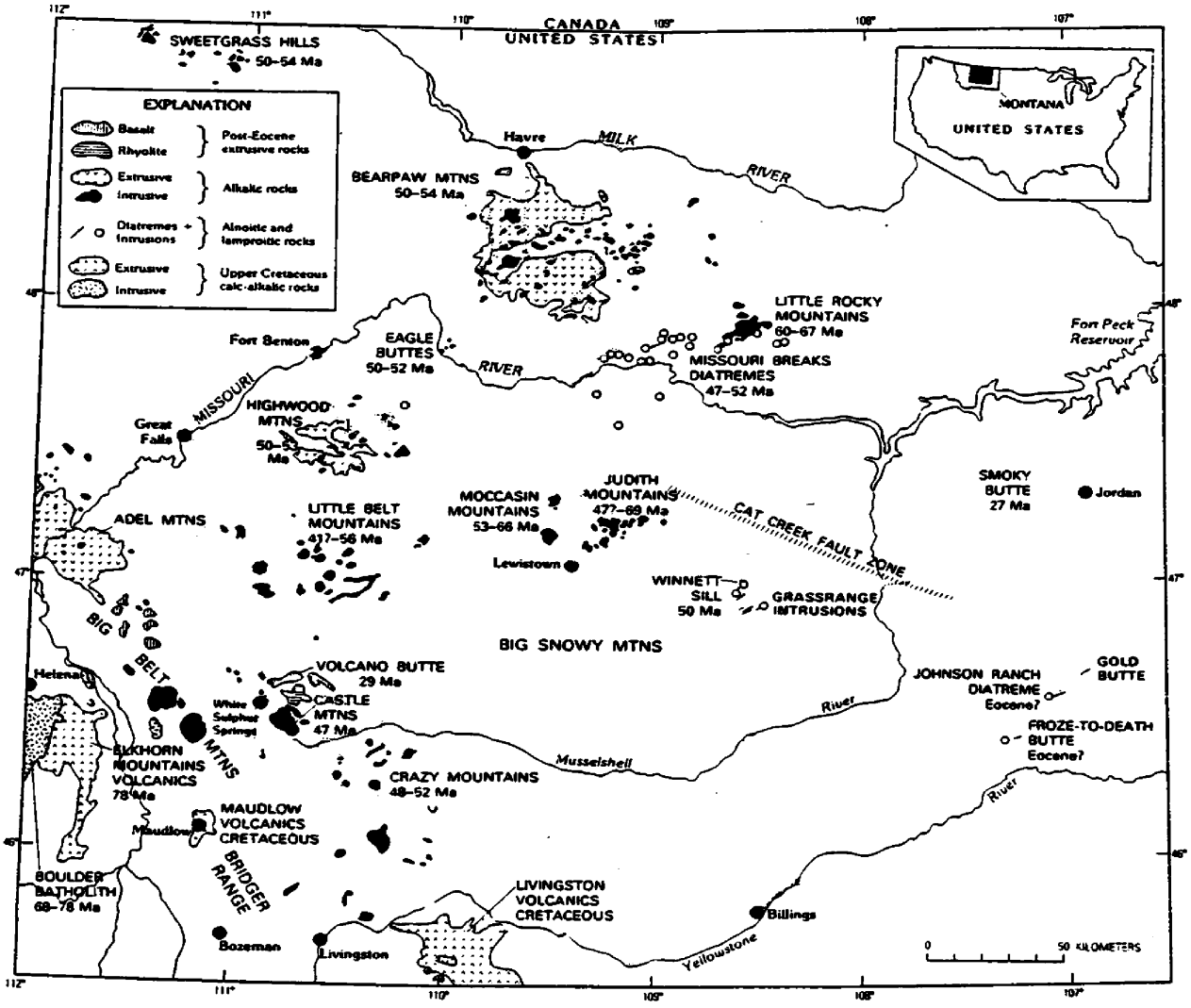

Figure 1 - Igneous rocks of central Montana modified from Hearn 1989. The Adel Mountains are located just north of 47 degrees latitude along the Missouri River. The Elkhorn Mountains, previously considered outside the central Montana Alkalic Province, are located directly south of the Adel Mountains. The Bearpaws and Highwoods which are well known for shonkinite melts and magma mixing and mingling are northeast from the Adel Mountains.

truncated and sloping boundary of the Wyoming Craton at the edge of the Adel Mountains is mimicked to the north by the anomalously high potassium mantle beneath central Montana (see Figure 14). Partial melting of the less potassic mantle beneath the Wyoming Craton permits generation of a basaltic magma whereas partial melting of the high potassium mantle, to the northeast, produces shonkinitic melts. A hypothetical model which accounts for the described relationships involves overlapping different mantle compositions where partial melting of "each" mantle at a range of depths can simultaneously produce both shonkinitic and basaltic melts. Such a model would predict increasing proportions of basaltic magma (or less alkaline magma) to the south. Alkalinity should increase to the north where the high potassium mantle dominates. Evidence for such a hypothesis is somewhat tenuous. However, the Elkhorn Mountains just south of the Adel Mountains reveal a combination of high potassium rocks (shonkinite) with low potassium rocks (basalt to alkalic basalt).

Chapter 1-2

THE CENTRAL MONTANA ALKALIC PROVINCE

The Adel Mountains lie near the southeastern end of a late Cretaceous to Eocene volcanic zone that extends through much of central Montana. Anomalous concentrations of potassium and sodium within the volcanic centers has led workers to classify the region as the Central Montana Alkalic Province or High Potassium Province (c.f.: Hearn et al. 1991, Pirsson 1905, Lyons 1944). The Adel Mountains lie 40 miles north of Helena along Route 15 (Figure 1).

The province is composed of late Cretaceous to early Eocene volcanic centers that produce alkalic mafic and felsic subalkalic magmas. Alkalic magmas are generally produced by rift faulting associated with crustal extension graben environments such as the East African rift valleys or the San Rafael Swell in Utah (Delaney 1997), or areas over the deep part of the subduction zone behind the main volcanic arc. However, there appears to be no clear correlation between such tectonic environments and the central Montana alkalic province. The isotopic signatures span the boundary between crustal and mantle source rocks with $^{87}Sr/^{86}Sr$ values ranging between 0.703-0.709 (Irving and O'Brien 1991). Irving and O'Brien interpret the disparity between isotopic values as assimilation of the Wyoming craton lithospheric mantle keel by asthenospheric melts. Other workers in the region have recognized high-potassium peridotite inclusions in volcanic rocks and suggest a high-potassium mantle source for the generated magma (Hearn et al. 1991).

Although previously controversial, the presence of an anomalously high-potassium mantle to produce the highly alkaline magmas characteristic of the region is becoming widely accepted. Factors controlling the generation of shonkinitic melts include the composition and volume of a mineral source, and the pressure and temperature where the melts are generated (Wilson 1994, p. 58). Unique melts such as shonkinite are interpreted to form by partial melting of phlogopite-bearing phases within the mantle at substantial depths (Hyndman 1985, p. 409).

Few geographic trends are noted within the central Montana Alkalic Province, although a general northeast line can be discerned between the three primary volcanic centers; the Adel Mountains, Highwood Mountains, and Bearpaw Mountains. However, associations beyond rudimentary spatial geography between these three centers are not clear. The primary relationship between these three volcanic centers involves the dominance of shonkinite and recent documentation of magma mixing and/or mingling in each locality.

Recent studies of the Bearpaw Mountains suggest that magma mixing and mingling at depth produces shonkinite inclusions in latite, latite dikes in shonkinite, and continuous petrographic and chemical gradation between the two magmatic phases (Tureck-Schwartz 1992, Hearn 1989, Hyndman et. al 1988). Mingling is clearly evident in both field and petrographic observations. Thin sections show olivine grains from the shonkinite magma reacting with a siliceous latite magma to produce disequilibrium features such as reaction rims of orthopyroxene, clinopyroxene, and biotite (Tureck-Schwartz 1992). This observed reaction strongly suggests magma mixing as a primary

hypothesis for the generation of the Bearpaw Mountains (Hyndman and Tureck-Schwartz 1992).

In the Highwood Mountains, evidence for magma mixing between early latite and high potassium mafic to felsic igneous rocks is suggested by mixed phenocryst assemblages and complex compositional zoning within olivines, clinopyroxenes, and mica phenocrysts (McCallum et. al 1989).

Chapter 1-3

PREVIOUS STUDIES IN THE ADEL MOUNTAINS

Through mapping, petrography, and chemical analyses, Lyons (1944) described the main characteristics of the Adel Mountains volcanic rocks. The Adels are primarily known for the radial dike swarm originating from the Three Sisters Stock and visible for several miles to the north of the main volcanic center (Hyndman and Alt 1987, Beall 1973). The Adel Mountains are overlain in part, to the southwest, by the Dearborn Ranch Thrust Fault which is associated with the Rocky Mountain Disturbed Belt. The volcanic rocks unconformably overlie the Cretaceous Two Medicine Formation (Beall 1973). The volcanic rocks were mapped in some detail by Schmidt (1977), who describes four primary units in stratigraphic succession. Trachybasaltic breccias and lava flows form the basal unit. These are overlain by latitic breccias and lava flows, and thin lacustrine deposits. The sequence is capped by a thick volcanic conglomerate sequence. A high angle fault runs through the western portion of the volcanic pile. This results in greater exposure in the uplifted block (Beall 1973). The present study, concentrated in the well exposed western fault block, primarily involves alkali basalt, shonkinite (or trachybasalt as described by Beall 1973), syenite veinlets, and latite intrusions.

Schmidt (1977) produced a series of detailed cross sections through the volcanic pile and interprets the latitic breccias and flows to be interlayered with the trachybasalt. He infers the trachybasalt to be far more voluminous than the latitic flows, and hypothesizes maximum trachybasalt thicknesses of up to 1,500 feet. The latitic breccias and flows have a maximum thickness of 200 feet.

The age of the volcanic rocks has been determined by K-Ar methods as late Cretaceous (71-81 Ma) (Sheriff and Gunderson 1990). Harlan (1991) suggests that this age can be further constrained to 73.6 ± 0.7 Ma based on $^{40}Ar/^{39}Ar$ dates from two biotites and one hornblende from a crosscutting intrusion that is interpreted to mark the termination of volcanism. Eruptive occurrences spanned 1-3 My.

Chapter 2-1

FIELD AND PETROGRAPHIC DESCRIPTIONS

Exposures of intrusive and extrusive volcanic rocks are prominently exposed along road cuts on Rt. 15 north and the Frontage Road following the Missouri River. The road cuts vary in size with the largest outcrop exposing approximately 50 vertical meters of rock. Horizontally, the road cuts extend several hundred meters (Plate 1). From a distance, it is possible to see large, felsic dikes crosscutting a mafic host.

Crosscutting relationships suggest a fairly consistent crystallization sequence which is inferred as follows: 1) Shonkinite and/or latite were erupted and intruded, 2) basalt intrudes previously crystallized shonkinite while a new generation of shonkinite intruded and formed mingling relationships between the basalt and shonkinite magmas, 3) several generations of shonkinite and/or hybrid magma continued to be intruded forming an intricate dike series, 4) syenite intruded. These relationships are easily discernable in Plate 2 and are described in detail below.

All samples from the Adel Mountains plot within the alkaline field and are clearly enriched in potassium (Figure 2). The present study tentatively defines four rock types based on field occurrence, petrography, and K_2O content. They include; 1) alkali basalt, (K_2O = less than 2.52 weight percent), 2) early, hematite-bearing shonkinite, and crosscutting shonkinitic dikes, (K_2O = 4.38-5.65 weight percent), 3) latite/monzonite, (K_2O = 2.96-3.73 weight percent), and 4) felsic meandering veinlets of syenite, (K_2O = greater than 6.08 weight percent) (see Appendix A). LeMaitre's igneous rock

Plate 1 - Outcrop 1. A view of a road cut to the east across the Missouri River. Notice the weathering shonkinite pillars and the more felsic late stage shonkinite dikes which are sub-parallel to Frontage Road.

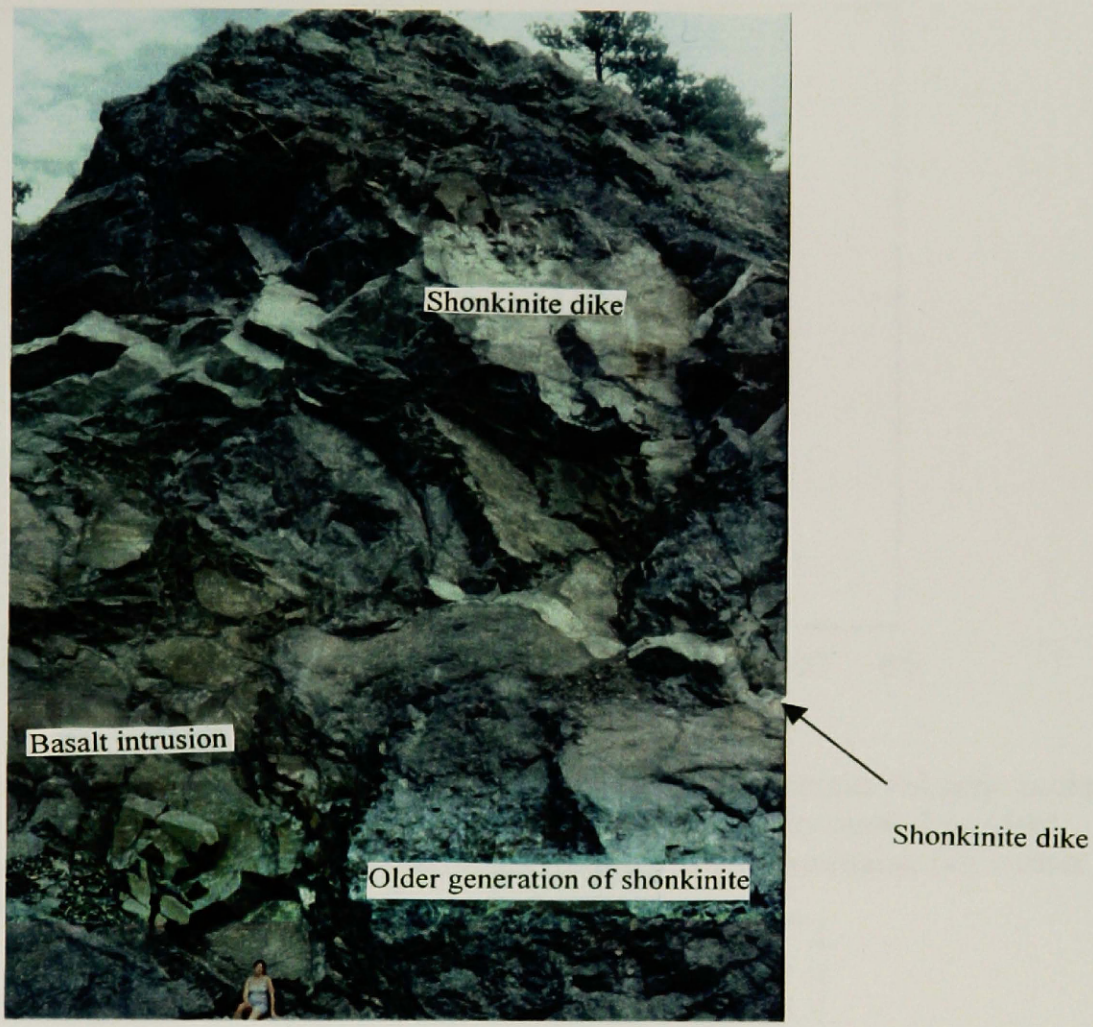

Plate 2 - Crosscutting relationships are evident in well exposed outcrops of the Adel Mountains. Note the multigenerational shonkinitic dikes which are crosscut by basalt. The oldest host rock weathers red and is described as a hematite bearing shonkinite.

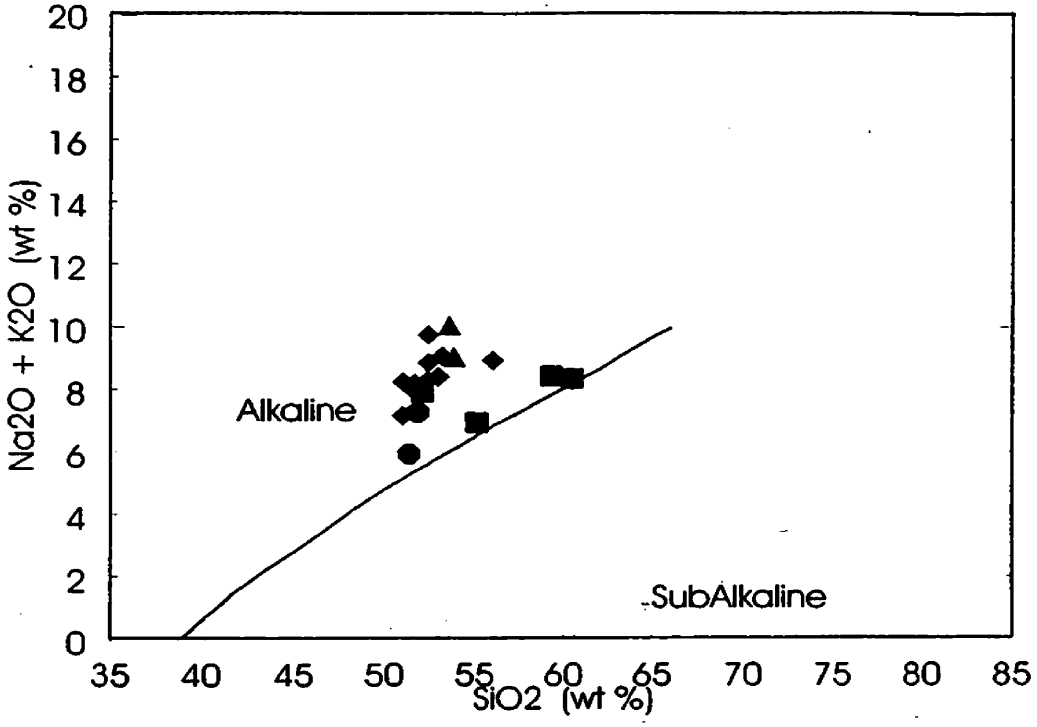

Figure 2 - Alkaline versus subalkaline distinction for the Adel Mountain volcanic rocks. Circles=basalt. Squares=latite. Diamonds=shonkinite. Triangles=syenite. Modified from Irvine and Baragar (1971). Note all samples from the Adel Mountains fall within the alkaline field.

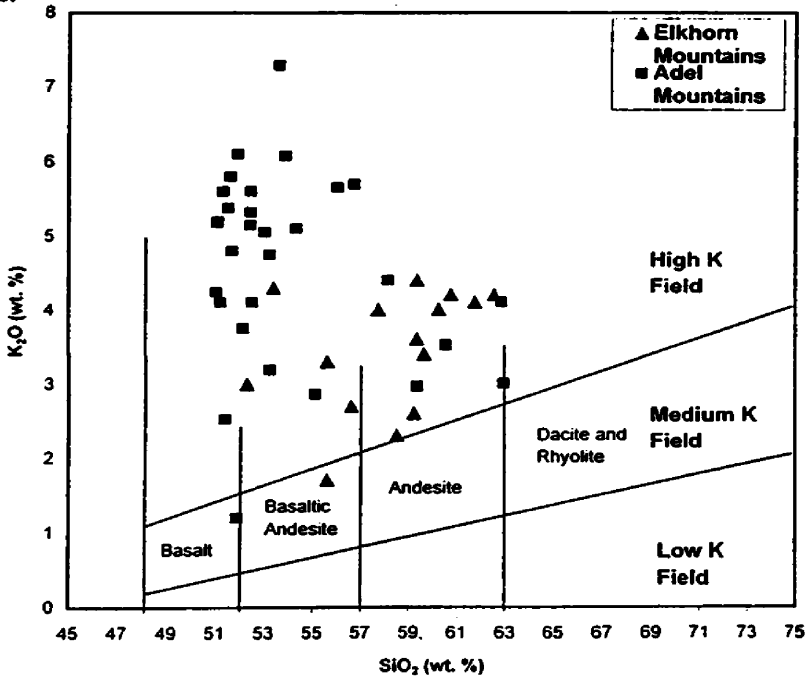

Figure 3 - Potassium versus silica classification for the Adel Mountains and the Elkhorn Mountains to the south. Elkhorn Mountains analyses from Rutland 1985. Most samples from both regions fall within the High-K field. A few fall within the Medium-K field and may have different origins. Diagram modified from LeMaitre 1989.

classification defines several fields based on potassium versus silica content (Figure 3). Most samples fall within the high potassium extensions from the basalt to basaltic andesite fields making distinction between groups difficult. Other classification schemes are equally ambiguous for the separation of rock types as described above. Distinct groups are evident when samples are plotted on an Na-K-Ca triangle (Figure 4). Latites are generally more sodium-enriched than the other rock types with the exception of a few shonkinite samples. It should be noted that distinction between groups is rather arbitrary and, as is clearly evident in many of the following diagrams, the rocks of the Adel Mountains plot close to one another which may suggest that a continuum of compositions exists. Each group is discussed in detail below based on field descriptions and chemical relationships.

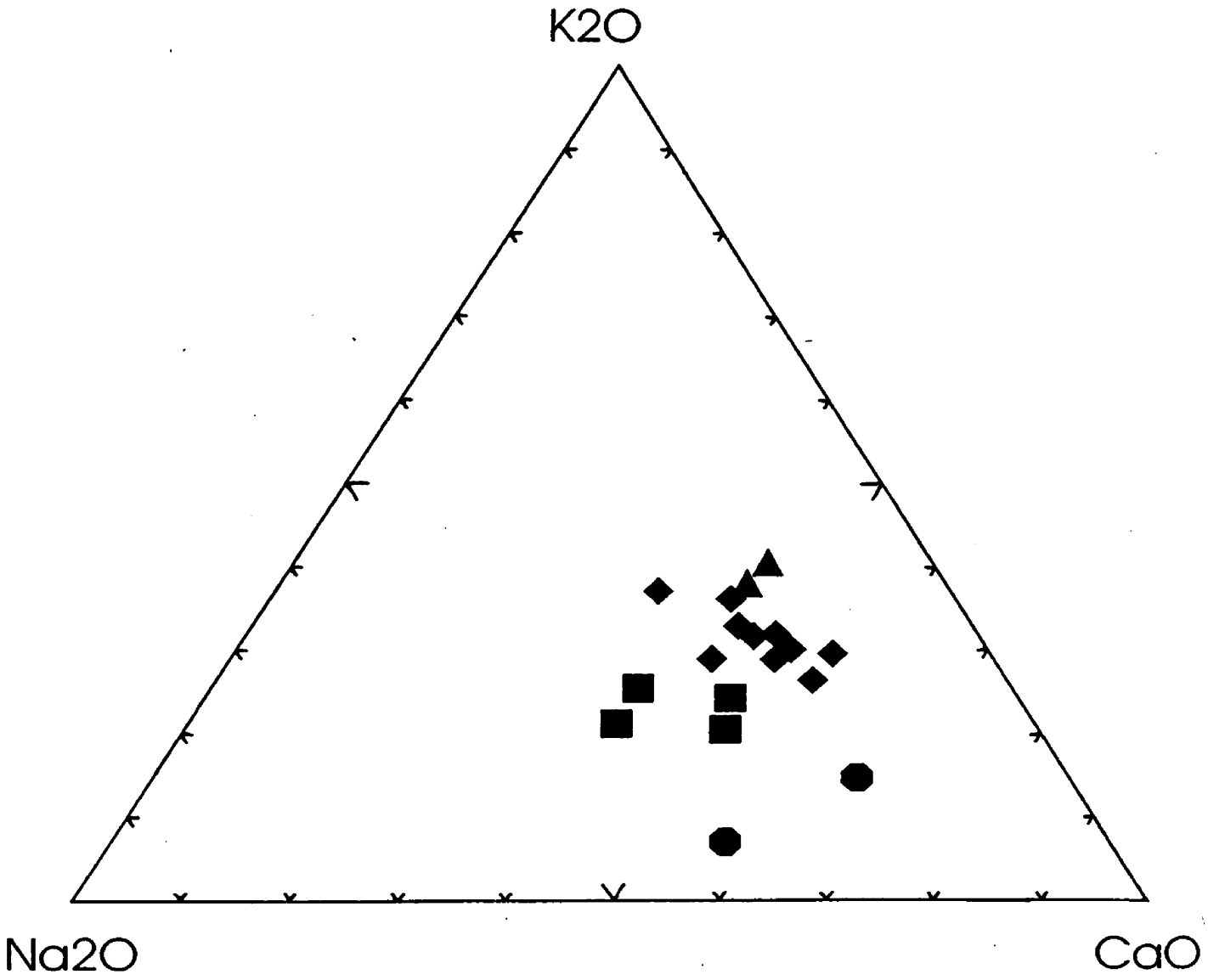

Figure 4 - Na-K-Ca classification triangle for Adel Mountains samples. Circles=basalt. Squares=latite. Diamonds=shonkinite. Triangles=syenite. Note the clear separation of rock types and the distinct location of basalt away from the primary rock cluster which may suggest different source rocks.

Chapter 2-2

ALKALIC BASALT

The most mafic of the Adel suite, alkalic basalt is apparent along Frontage Road and appears as isolated dikes which cut across host shonkinite (Plate 2). In outcrop, alkalic basalt weathers brown and is easily distinguishable from associated shonkinite. Although volumetrically minor, the alkalic basalt may be genetically related to the Elkhorn Mountains volcanic rocks which were previously thought to lie outside the central Montana Alkalic Province.

A few phenocrysts of augite are visible in hand specimen, surrounded by a fine grained dark matrix. In thin section, abundant plagioclase, altered olivine, isolated calcite, magnetite, and auxiliary apatite constitute the groundmass. Augite is the most abundant phenocryst phase. Most crystals are euhedral to subhedral and demonstrate prominent normal zoning. This suggests a continually changing host magma composition (Plate 3). Intergrown augite crystals form some glomerocrysts. Olivine grains are rounded and completely altered to iddingsite and serpentine. Plagioclase laths are well twinned forming euhedral to subheddral grains. The exact order of crystallization is difficult to discern; however, the abundant and exceptionally large augite phenocrysts are inferred to be the first to crystallize in order to have the most time to develop.

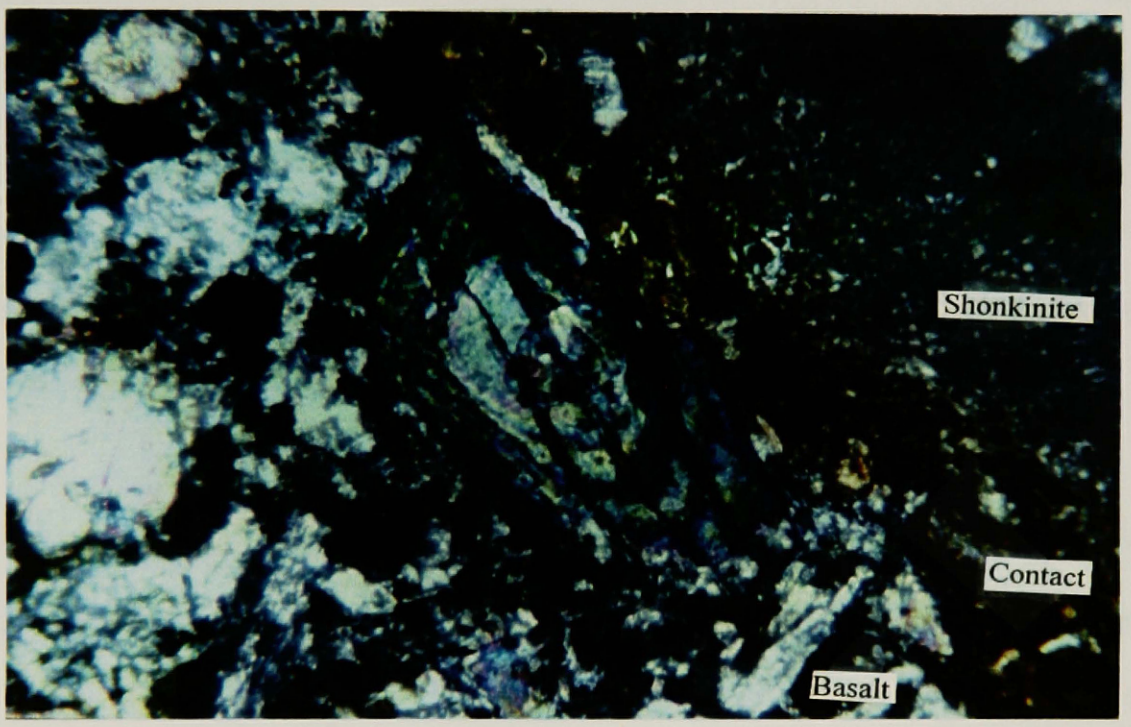

Plate 3 - Photomicrograph, in crossed polars, of zoned augite in host basalt. The augite grain appears to be truncated against the later intruded shonkinite dike which may suggest that the basalt was fairly well crystallized at the time of shonkinite injection. No mingling relationships were observed at this locality. Field of view is approximately 1mm.

Chapter 2-3

LATITE

Latite in the Adel Mountains is technically a latitic basalt or monzogabbro although for simplicity, I use the term latite after its use by Schmidt (1977). Although it makes up only 10% of the total volume, latite is the second most abundant rock in the volcanic pile. It occurs primarily as a massive, fine grained body bounded on all sides and cross-cut by shonkinite. Other minor exposures preserve irregular borders between the latitic intrusion and early, host shonkinite; this may suggest minor mingling during latite emplacement.

In hand sample, latite is medium gray, to grayish green and has sparse phenocrysts of clinopyroxene(?) and/ or hornblende. In thin section, a minor concentration of small laths of hornblende exhibit brown pleochroism in plane light. Such hornblende color is often associated with shallow volcanic rocks. The groundmass of all latite samples consists primarily of feldspar (plagioclase and sanidine) in varying proportions. Accessory magnetite, hematite, and epidote are also present. As is evident in Figure 4, latite is compositionally uniform and distinct, and demonstrates the relative abundance of plagioclase present in these rocks.

Chapter 2-4

SHONKINITE

Shonkinite (also referred to as shoshonite in the literature, although technically a different rock) is a salite-bearing, potassium-rich rock with K_2O contents averaging 3.36 weight percent (Hyndman 1985, p. 386). In the Adel Mountains, shonkinite makes up approximately 80% of the volcanic pile with an inferred maximum thickness of 450 meters; it occurs as early flows, and as dikes which are interpreted to form in several generations (Schmidt 1977). Easily distinguishable weathered pillars of shonkinite are exposed in grandeur throughout the pile making the Adels one of the most scenic regions in central Montana. In hand sample, euhedral phenocrysts of salite ranging from 1-10mm in length are immediately apparent in a groundmass primarily composed of alkali feldspar.

Early erupted shonkinites are very altered and weather red due to the abundance of hematite. Calcite is also abundant in the highly altered rocks. Calcification may in part be related to re-precipitation from altered plagioclase. Later generations of dikes are fairly fresh and are dark gray to green. Contacts with the host rock result in a whitish rim several millimeters thick (Plate 4 and Plate 5). Weathered surfaces are white to light gray (Plate 1). Generations of shonkinite dikes cross-cut all other rock types in the volcanic pile with the exception of syenite veinlets which are not associated with any dikes. Although variation in orientation is substantial, most dikes are oriented sub-parallel and trend north-south.

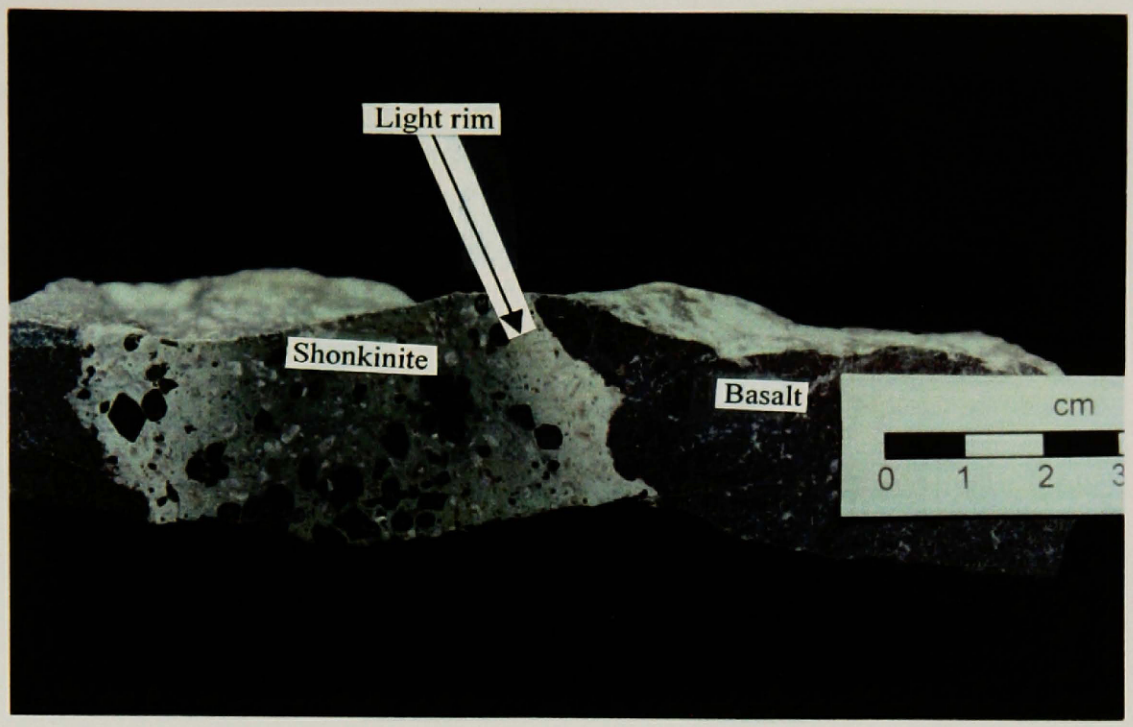

Plate 4 - Mingling relationships between basalt and shonkinite. Note the light rim which follows the contact and may be related to cation exchange between the two magmas prior to crystallization.

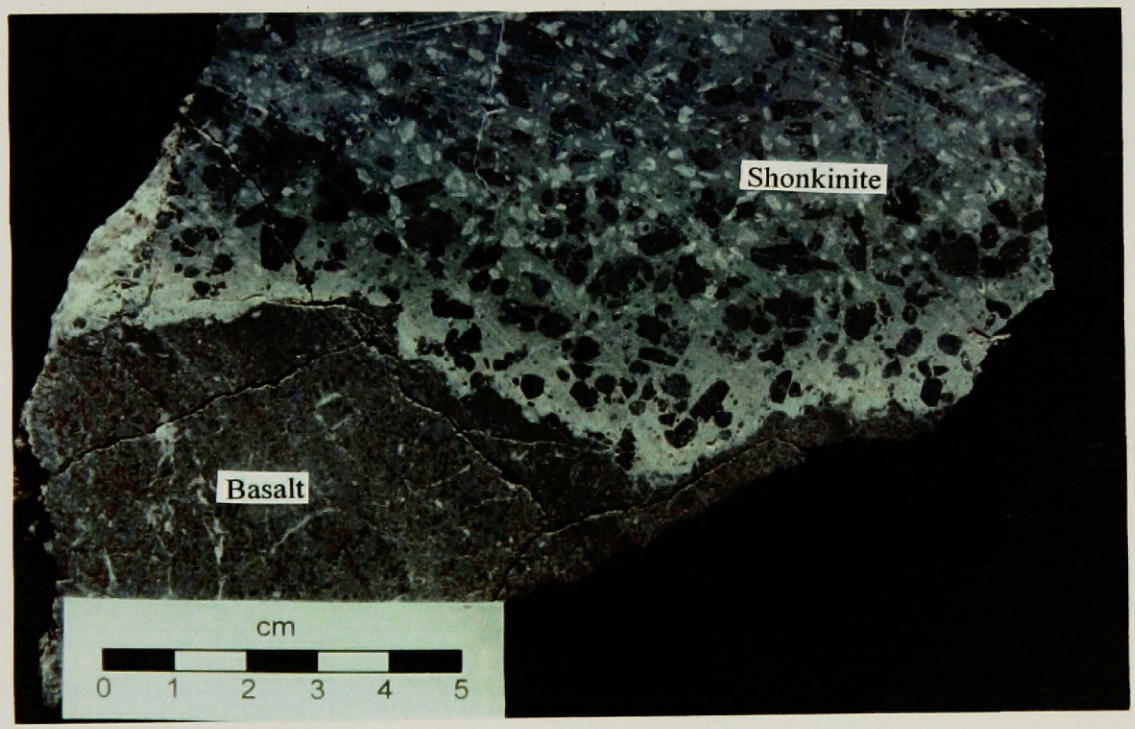

Plate 5 - Mingling relationships between basalt and shonkinite. Note the highly irregular border and some fine stringers of shonkinite within basalt.

Petrographically, shonkinite is porphyritic in texture with salite and smaller olivine phenocrysts contained in a medium to fine grained groundmass consisting primarily of sanidine, plagioclase, salite, olivine, magnetite, calcite, apatite, and alteration minerals. Chilled shonkinite is located near mingled borders with either earlier formed shonkinite or basalt. Petrographic differences between rim and mingled shonkinite and core shonkinite vary. Plate 3 and Plate 6 suggest that evidence for mingling is not only apparent in outcrop scale, but also petrographically. Plate 6 shows basalt being injected in to the shonkinite melt to form a bulbous, mingling feature. Note the zoned augite grain in basalt in Plate 3 which is truncated by the shonkinite contact. This suggests that basalt was partially crystalline at the time of shonkinite injection. There must have been a temperature difference between the two magmas causing shonkinite to chill against basalt. However, the variation was small enough to still allow for interaction between the magmas. Note the distinct grain size discrepancy between the basalt and shonkinite groundmass which again suggests the shonkinite did not have a lengthy time to mingle or mix with host basalt.

Salite grains close to the contact exhibit much higher levels of resorption and thin reaction rings which represent chemical interaction with the proximal magma. Biotite is present in shonkinite only near the dike rims and is pleochroic reddish brown in the Z direction and light yellow along the X axis. Calcium from plagioclase mobilized to form a small concentration of calcite in the groundmass. Petrographic mineral identification in the chilled groundmass is impossible.

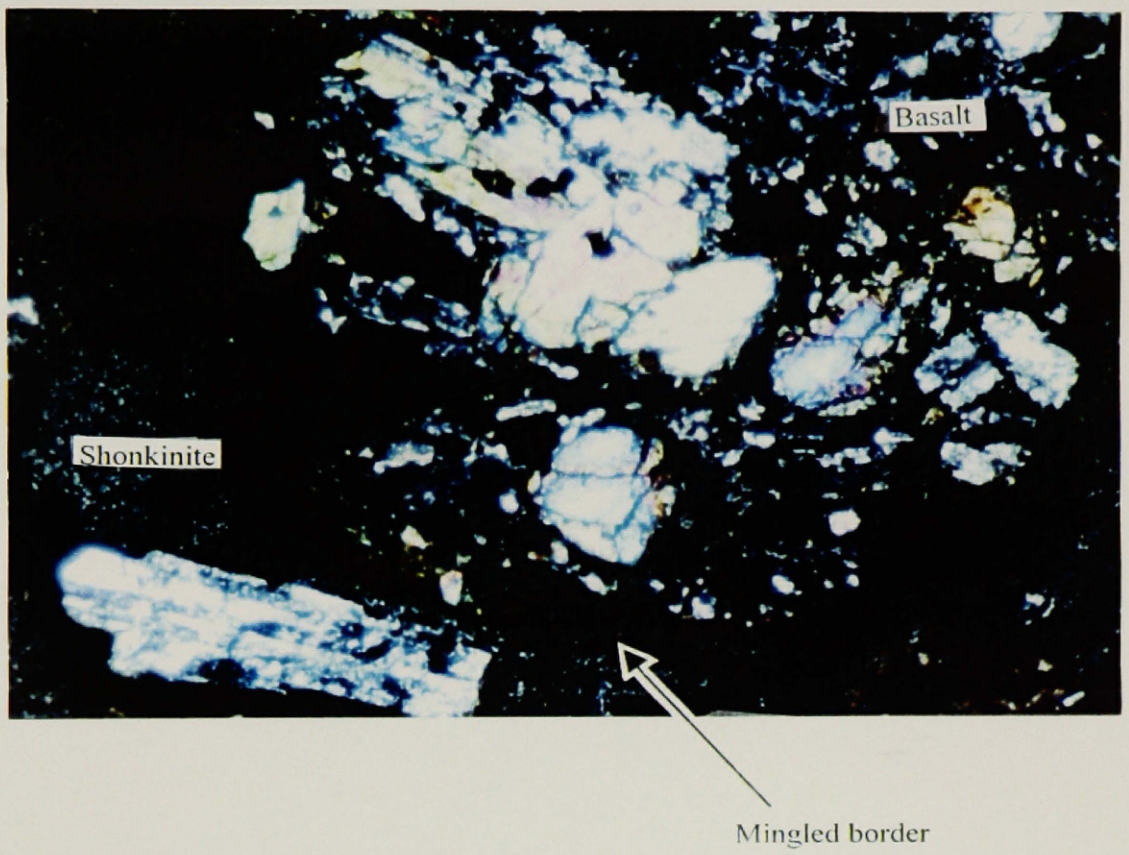

Plate 6 - Crossed polars view of medium grained basalt mingled as a bulbous mass with shonkinite host. Field of view approximately 2mm.

Euhedral salite grains which form near the core of a shonkinite dike demonstrate significantly less resorption. A few salite grains have been embayed by the groundmass. The groundmass within the center of the dike is coarser and consists primarily of sanidine with some plagioclase and alteration minerals.

Chapter 2-5

SYENITE

Associated strictly with host shonkinite, syenite is volumetrically the smallest component of the volcanic pile. Syenite forms small, leucocratic veinlets which meander in stark contrast through darkly weathered shonkinite (Plate 7). Note the anastamosing veinlets which are characteristic of immiscibly derived syenite. In some localities, accumulations of salite crystals are found confined to the center of syenite veins, perhaps by flowage differentiation (Plate 8).

Petrographically, sanidine is the primary component in the groundmass of syenite. The percent sanidine is difficult to discern in such a fine grained rock. The difference in sanidine content between syenite and host shonkinite is most apparent when the rocks are stained with hydrofluoric acid and sodiumcobaltinitrite (Plate 9). Note the high abundance of yellow stain which reflects the potassium content in the small syenite veinlets.

Plate 7 -Syenite veinlets in a mafic host. Hammer for scale. Veinlets and globules support liquid immiscibility as a source for the generation of syenite.

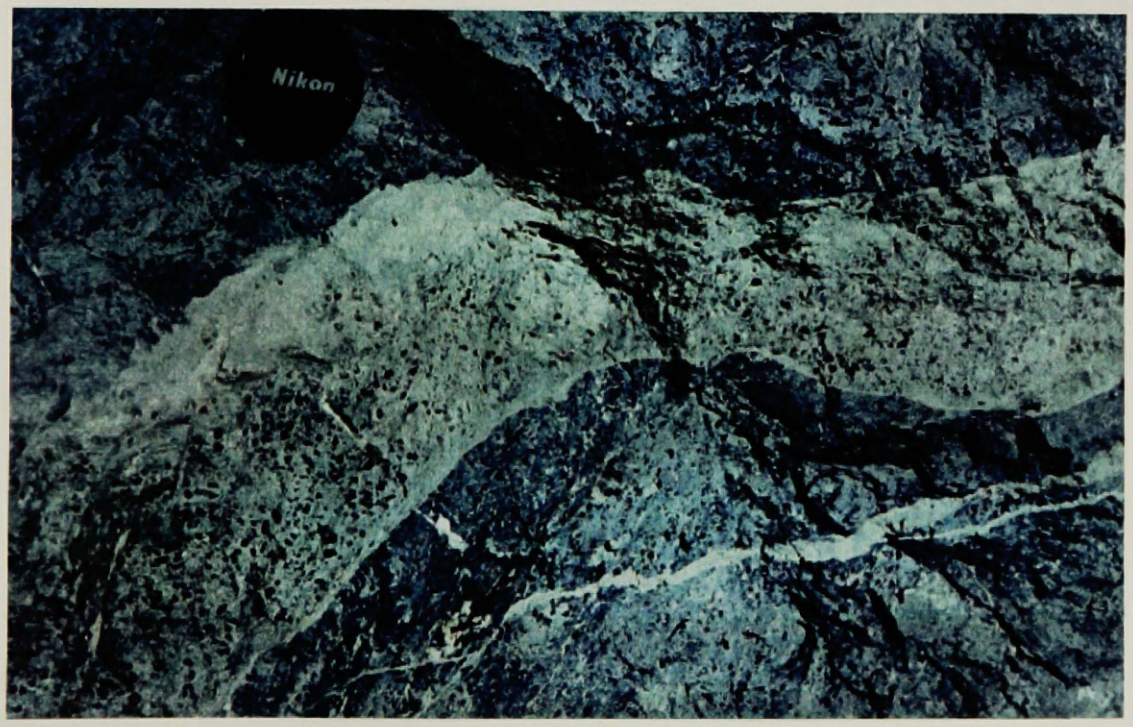

Plate 8 -Salite accumulation in syenite veinlets. Identical mineral species in the felsic and mafic rocks is also suggestive of immiscible separation. Both shonkinite and syenite are primarily sanidine and salite.

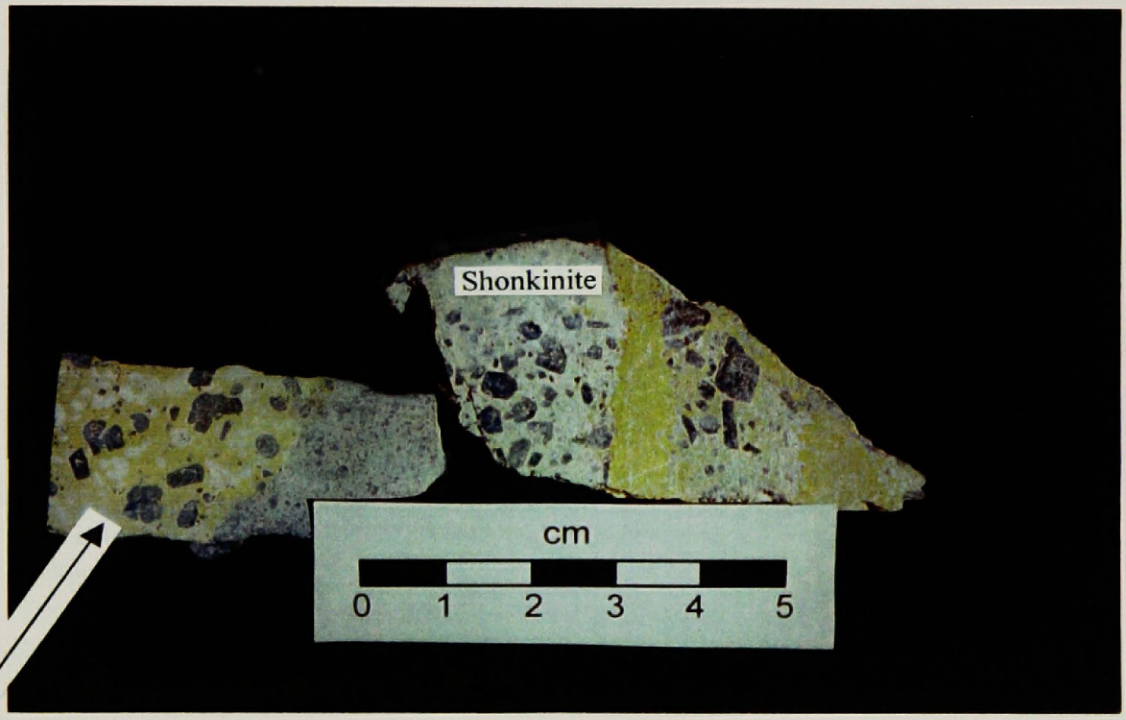

Plate 9 -Potassium feldspar stained yellow with hydrofluoric acid and sodium cobaltinitrite to accentuate potassium concentration in syenite veinlets. Note the large salite phenocrysts in both rocks.

Chapter 3

PROPOSED MODELS FOR OBSERVED ASSOCIATIONS

Three primary models potentially account for the compositional variation found throughout the Adel Mountains volcanic rocks; 1) magma mixing and mingling, 2) differentiation, both through fractional crystallization and liquid immiscibility, and 3) assimilation of country rock. Outlined below is a brief description of each model as well as the assocaited field, petrographic, and chemical criteria for distinguishing between them.

Magma Mixing and Mingling

Although the term mingling is a recent developement, there has been concrete documentation of mingling dating back to papers by Wilcox (1969) and Sparks and Sigurdsson (1977). Mingling represents physical interaction without chemical homogenization. Mixing, in contrast, implies a complete chemical homogenization between the magmas. Field evidence for magma mixing or mingling includes mutually crosscutting, or gradational relationships between the mafic and felsic rocks with inclusions of each phase occurring within the other. Petrographically, clinopyroxene or olivine in contact with a siliceous magma demonstrate disequilibrium features such as reaction rims of pyroxene, hornblende, and/or biotite, embayed crystals, and oscillatory zoning (Tureck-Schwartz 1992). Variable phenocryst compositions of a single mineral species also indicate mixing. Major-element chemical analyses produce linear trends on Harker diagrams with a continuum of compositions between the two magmas, when shonkinite and latite are end members.

Differentiation

A second hypothesis involves differentiation either through fractional crystallization or liquid immiscibility. Fractional crystallization involves the physical removal of a crystalline phase or phases from the melt by gravitational settling or some other process. The amount of fractional crystallization that occurs depends on the magma rheology, phenocryst size, and density contrast between fractionationed crystals and melt.

Petrographic examination of a rock which has undergone differentiation demonstrates disequilibrium features such as normal zoning, oscillatory zoning, and inclusions of the fractionated phase or immiscible liquid within the host rock. In terms of chemistry, fractionated magmas plot as curved lines on oxide diagrams. Modeling of fractionation patterns based on the removal of individual crystalline phases produces clear trends for the path the residual magma should follow. Further evidence suggesting differentiation includes enrichment in the residual melt of Zr, Th, U, Rb, Ba, and Nb by approximately ten times the normal element quantities in a parent basalt (c.f.: Hyndman 1985, p. 118). Finally, syenite is the normal differentiation product of shonkinite, and the evolution of latite through this means would be highly improbable (Edmund 1980, Kuhn 1983). Differentiation of shonkinite in Shonkin Sag laccolith in the Highwood Mountains demonstrates a clear separation to syenite near the top of the section.

Another form of fractionation, liquid immiscibility is a thermal equilibrium process thereby negating the presence of chill zones within immiscible magmas. Mafic magmas

with concentrations of La and Ce greater than their associated felsic magmas are also characteristic of immiscible processes (Watson 1976). Furthermore, because two immiscible liquids must be in equilibrium with each other, they should produce the same crystalline phases assuming that the liquid does not continue to fractionate beyond the immiscible separation. Another indication of immiscibility is the distribution of titanium and phosphorous. During immiscibile separation, both elements concentrate in the mafic magma, whereas with crystal fractionation, phosphorous and titanium generally concentrate in the felsic phase (c.f.: McBirney 1993). Other evidence for immiscibility is similar to that of fractional crystallization as described above.

Assimilation

When a melt rises through the mantle and eventually reaches the lower crust, it selectively extracts certain elements by exchange from the crustal rock. These elements may be incorporated into the melt by chemical diffusion (Watson 1976). Bulk assimilation involves complete incorporation of a mass of the host rock into the magma and is much more common. Granitic crustal xenoliths, especially those with metasomatic reactions or intermediate compositions would clearly demonstrate the importance of assimilation in modifying the rising melt. The degree of assimilation depends on the temperature contrast between ascending magma and wallrock, the rate of ascension, and the fusion temperature of the wallrock and magma (DePaolo 1981). Generally, assimilation of granitic crustal rock within an ascending mafic melt would produce a magma enriched in felsic constituents. When plotted on a Harker diagram, the composition of magma modified by assimilation trends toward the composition of the

incorporated crustal rock; in this case, toward a granitic composition (c.f.: Tureck-Schwartz 1992). However, the ability of a silica undersaturated melt (either shonkinite or basalt) to assimilate the quantity of rock needed to produce a magma like syenite or latite is doubtful; it requires assimilation of an unrealistically large quantity of granite (Tureck-Schwartz 1992). Such a quantity would require an unlikely degree of superheat in the invading magma.

Chapter 4

EVIDENCE FOR MAGMA MINGLING

In order for magma mingling to occur, certain criteria must be satisfied. Magma mingling requires two separate magmas to be present in the same place and at the same time in order to become mechanically interwoven. Sufficient time with both molten would foster creation of a hybrid or intermediate composition of magma. Mingling usually occurs with one magma quenching against the cooler magma or with substantial viscosity differences and a short time period to keep the magmas from homogenizing as noted above (Plate 3 and Plate 6) (Frost 1987). Under special circumstances, magmas which are of similar composition and are injected deep in a volcanic pile through repeated pulsing may remain molten long enough to mechanically interact and preserve evidence of magma mingling before being completely quenched. Although a minor factor when considering the petrogenesis of the entire system, magma mingling is intricately interwoven into the history of the region and provides a foundation for determining sequential constraints on intrusive units.

In the Adel Mountains, magma mingling is preserved between generations of shonkinite flows and dikes, between shonkinite dikes and host alkalic basalt, and potentially between latite and shonkinite. Plate 10 and Plate 11 suggest that shonkinite and basalt were present simultaneously as magmas or at least were only partly crystalline during their interaction. Note the inclusion of basalt in the more felsic shonkinite (Plate 10), while in Plate 11, shonkinite appears to meander within the basalt host. Foster and Hyndman (1990) determined that a magma behaves as a ductile solid before it is 60

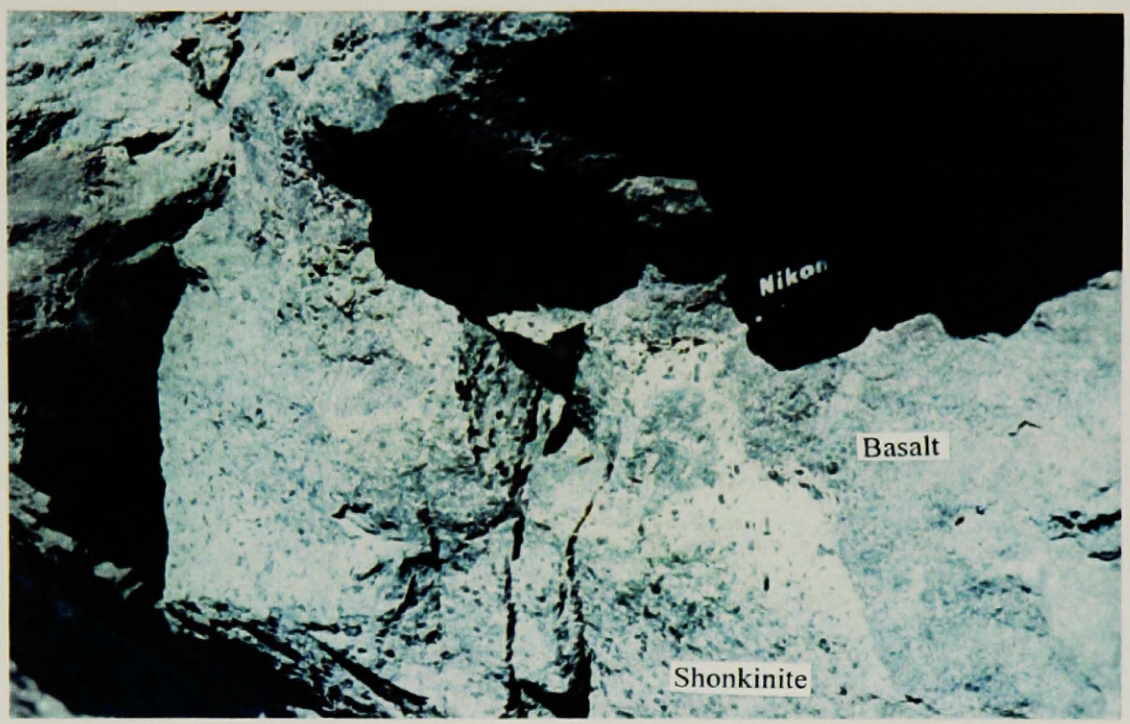

Plate 10 -Magma mingling between shonkinite and basalt. Note the irregular borders of the shonkinite dike and the incorporation of basalt magma as an inclusion.

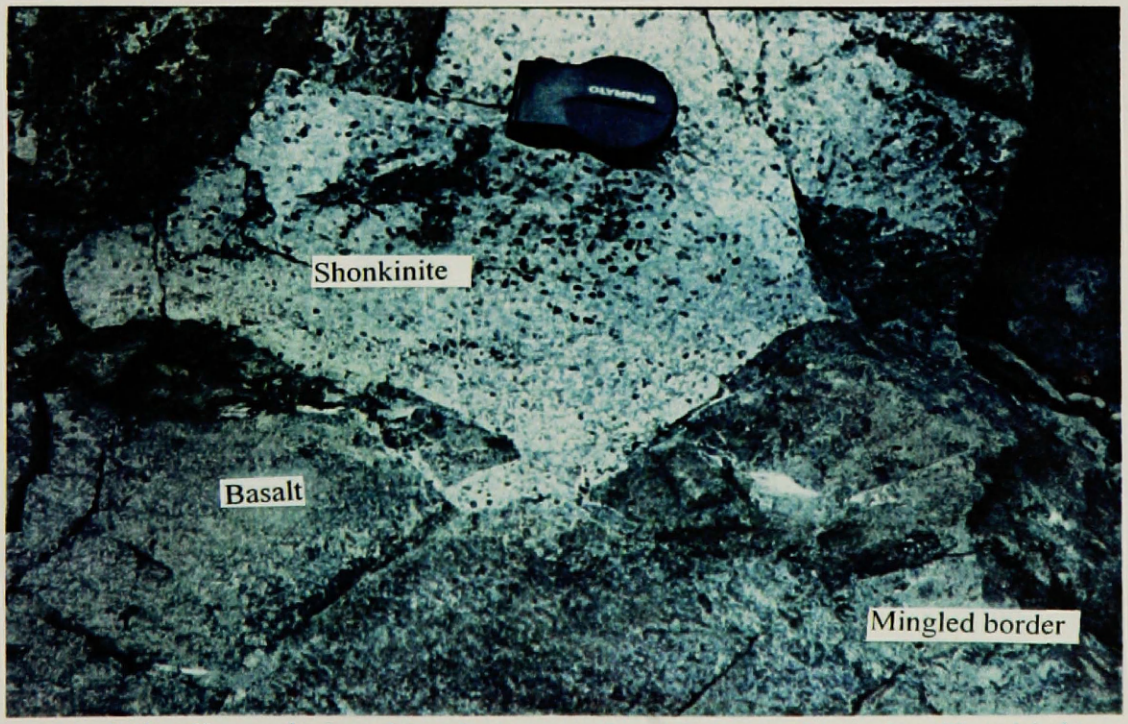

Plate 11 -Mingling relationships between shonkinite and basalt. Shonkinite meanders through the basaltic host.

percent crystallized. Therefore, it could sustain a fracture which would provide a conduit for magma injection. This supports field relationships that I see and confirms the potential for a partially cooled, crystalline magma such as host alkalic basalt or an early generation of shonkinite, to fracture and be injected by a hotter pulse of fresh magma and still be fluid enough to mingle. However, through detecting magma mingling, it is reasonable to assess that the intrusive period of these rocks was relatively short in order to maintain enough heat content to adequently insulate the injected magmas while they mingled with the host but not long enough to allow homogenization. Truncated swirls, the presence of chill zones, and the limited findings of such occurrences may suggest that the duration of mingling was fairly short.

Chapter 5-1

GEOCHEMICAL RESULTS AND ANALYSES

Thirty samples were analyzed by x-ray fluorescence (XRF) for major and trace elements. Thirteen additional chemical analyses are the result of work by Beall (1973) (Appendix A). These analyses are not incorporated in diagrams where field relationships are significant since detailed sample sites were not described by Beall (1973). Analysis accuracy is discussed in detail in Appendix B. As outlined above, three primary models for the observed relationships include magma mixing and mingling, differentiation, and assimilation. Geochemical analysis is one of the primary means to test the validity of petrogenic models. Although theoretically an interesting model, bulk assimilation of crustal basament rocks by mafic magma to form latite is not discussed further, in agreement with Tureck-Schwartz's findings that it was highly improbable. Magma mixing and mingling, and differentiation by both fractional crystallization and liquid immiscibility, are discussed below.

Chapter 5-2

GEOCHEMICAL MODELS FOR MAGMA MIXING AND MINGLING

As discussed in Chapter 3, if two magmas were to completely mix, a hybrid magma would form. Mingling emphasizes strictly mechanical interaction with lesser chemical homogenization. Therefore, magma mixing is the primary process to be tested by major and trace element chemistry. Both shonkinite and basalt are considered mafic end members when modeling mixing trends with latite. Each is examined independently.

Mixing as a petrogenic process is tested by inferring mafic end members and parent latites and determining if rocks of intermediate composition lie between the end members. Parent shonkinites and basalts are interpreted as those which exhibit a combination of relevant parameters: 1) minor alteration and contamination; 2) high MgO concentrations, 3) low L.O.I. (loss on ignition) values, and 4) low Na_2O concentrations (Appendix C). Note that the most magnesium-rich rock was not chosen as a parent shonkinite. The degree of alteration on this early formed shonkinite is apparent in the high proportion of zeolites and calcite present in thin section and also reflected in the anomalously high L.O.I. value. Parent latites were selected because they exhibit low L.O.I. and MgO values with slightly higher Na_2O numbers. The end member shonkinites and latites are determined by averaging groups of samples that fit the above guidelines.

The alkalic basalt with a high concentration of potassium is also the most magnesium rich making a single basalt end member difficult to discern. Since only two basalt compositions are available for analysis, these were averaged to yield the basalt

composition for mixing models. It is important to consider that the basalt samples may not be the "primitive" magma and are most likely a product of partial fractionation. This is evidenced by their relatively low Ni and Cr concentrations (see Appendix A). Rocks with low Ni and Cr values are inferred to have fractionated olivine and pyroxene. If fractionation has occurred, the melts are not primary. Because variation in element concentration is more extreme following fractionation, modeling without a true primitive magma is complex.

Alkalic Basalt as a Mafic Endmember for Mixing

The end of the mixing arrow is inferred as the most mafic composition for basalt. As with shonkinite, when examining Harker diagrams which delineate average basalt and average latite compositions, a few samples plot close to the proposed mixing line (Figure 5 a-i). Those which are close to the proposed mixing line tend to have higher silica values and may have a slightly different origin than their more silica undersaturated counterparts. Modeling of mid-crustal partial melt compositions is compatible with latite compositions observed in the Adel suite as is discussed below. Mixing between end member latite and basalt is plausible for some intermediate samples. Note tat if crystal fractionation and magma mixing both operate, the samples should lie off the mixing line towards the trend indicated for fractionation of augite or possibly olivine. This is plausible for TiO_2, FeO, CaO but not Na_2O and K_2O. These latter oxides may have moved by volatile diffusion.

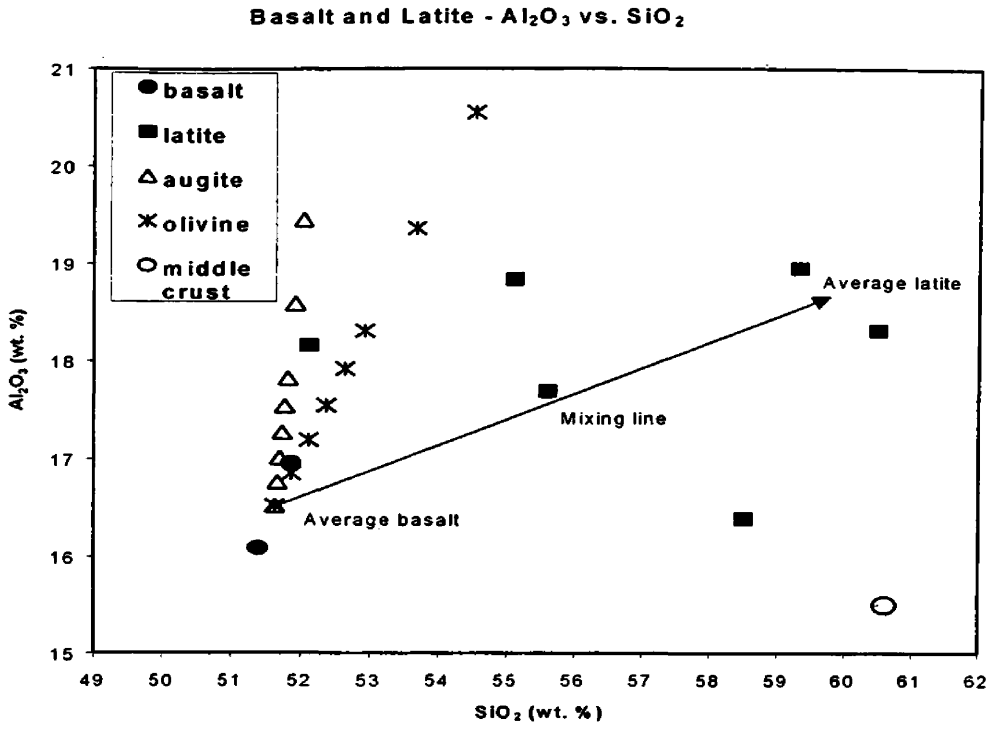

Figure 5a - Potential mixing of endmember basalt and latite. Incremental fractionation modeling of augite and olivine. See Figure 9 for a detailed explanation.

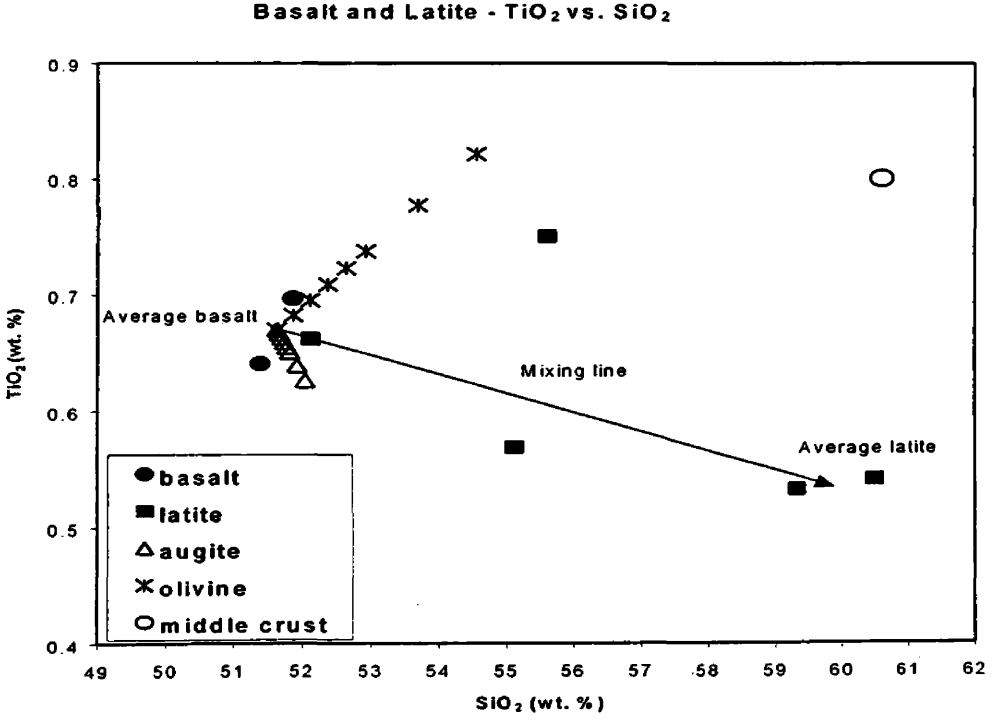

Figure 5b - Potential mixing of endmember basalt and latite. Incremental fractionation modeling of augite and olivine. See Figure 9 for a detailed explanation.

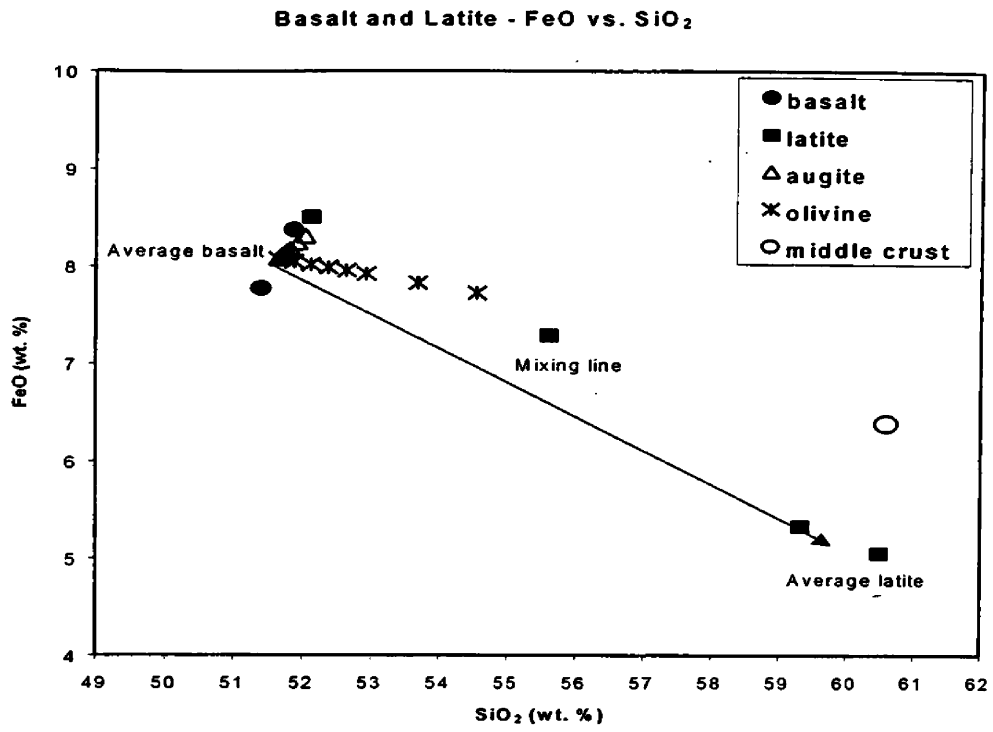

Figure 5c - Potential mixing of endmember basalt and latite. Incremental fractionation modeling of augite and olivine. See Figure 9 for a detailed explanation.

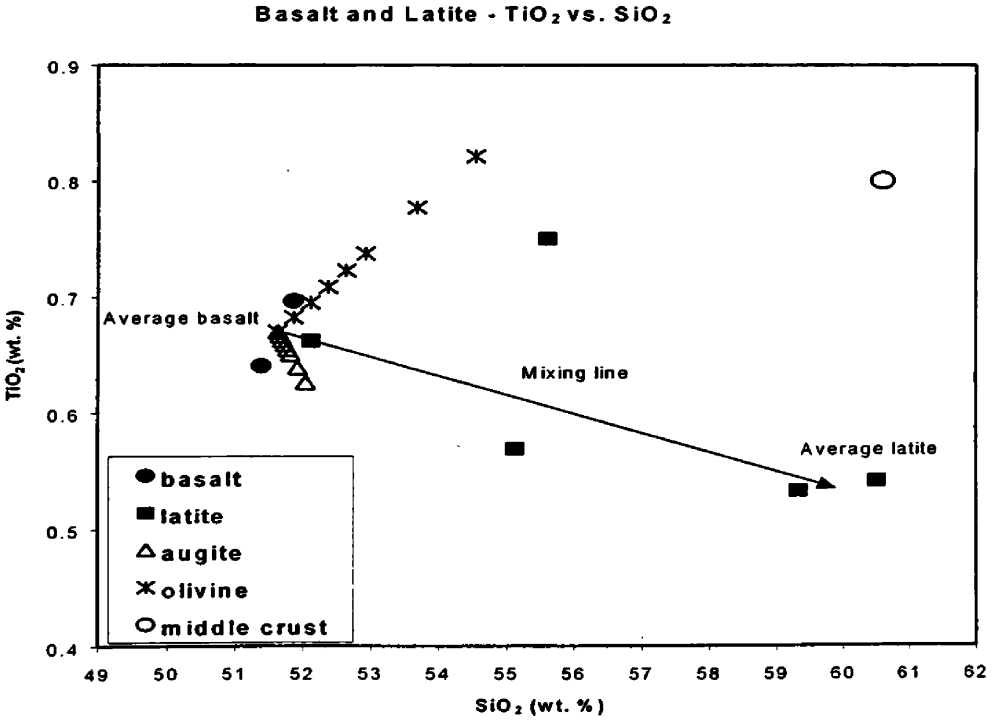

Figure 5d - Potential mixing of endmember basalt and latite. Incremental fractionation modeling of augite and olivine. See Figure 9 for a detailed explanation.

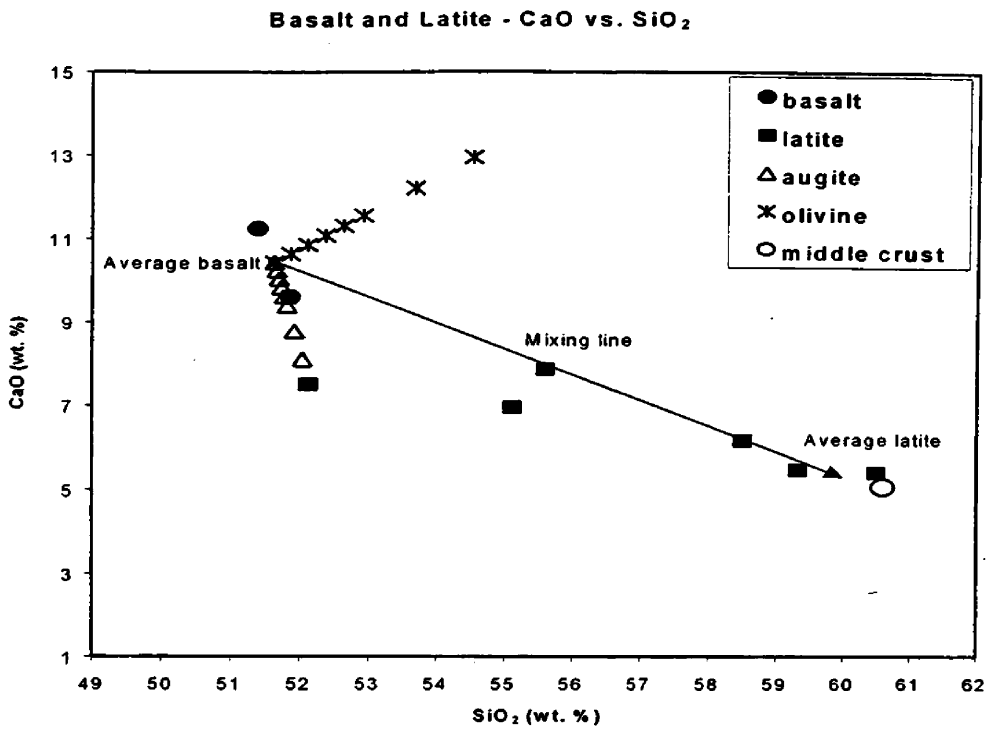

Figure 5e - Potential mixing of endmember basalt and latite. Incremental fractionation modeling of augite and olivine. See Figure 9 for a detailed explanation.

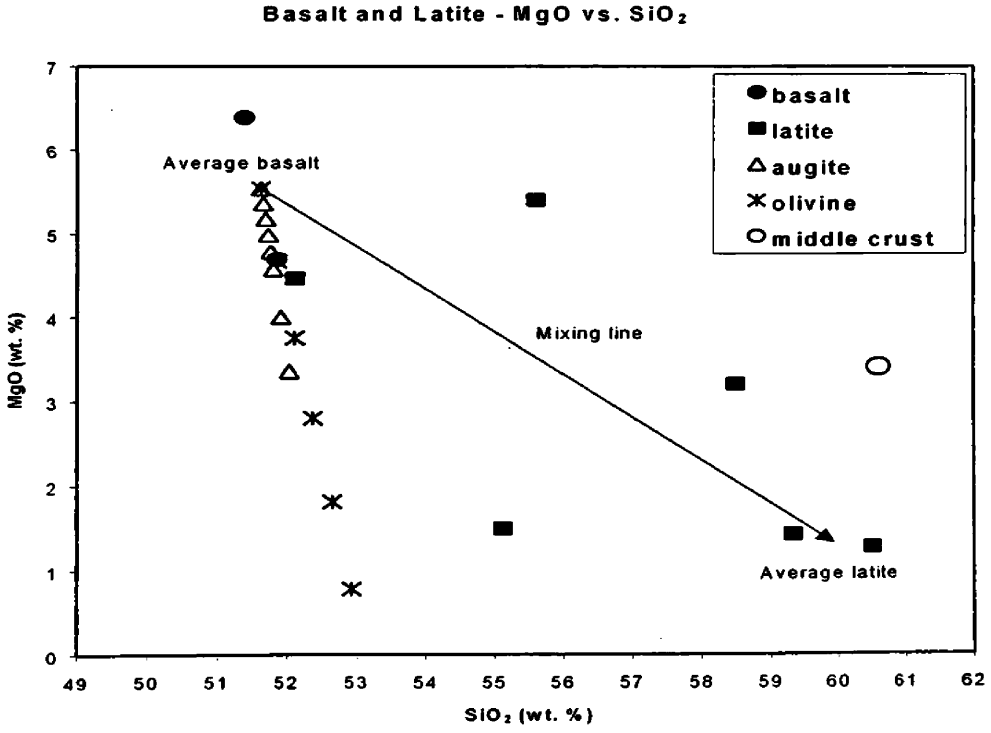

Figure 5f - Potential mixing of endmember basalt and latite. Incremental fractionation modeling of augite and olivine. See Figure 9 for a detailed explanation.

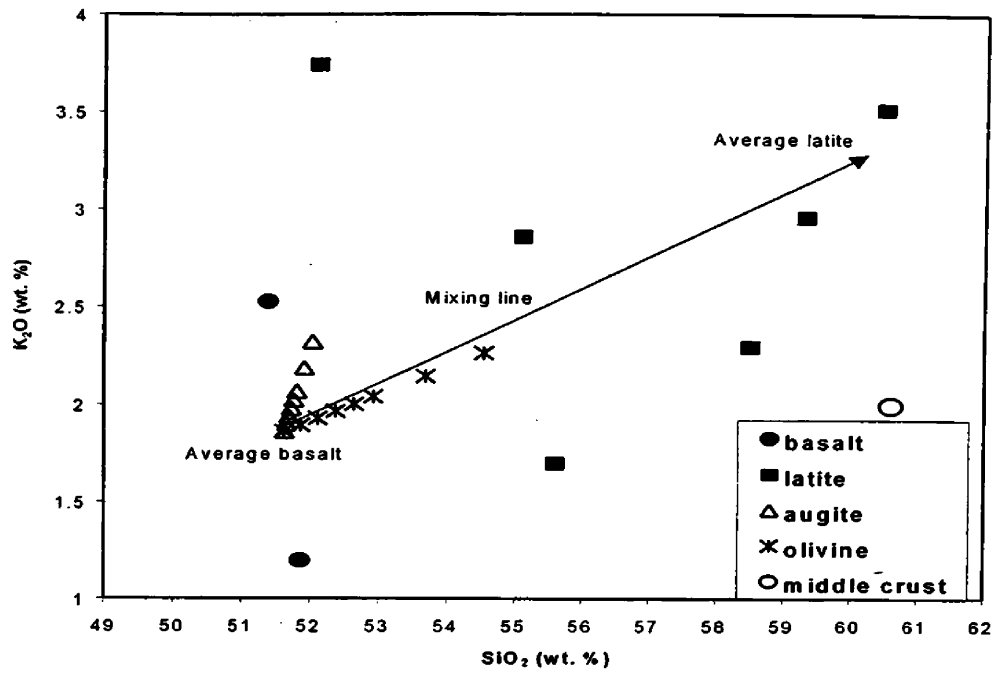

Figure 5g - Potential mixing of endmember basalt and latite. Incremental fractionation modeling of augite and olivine. See Figure 9 for a detailed explanation.

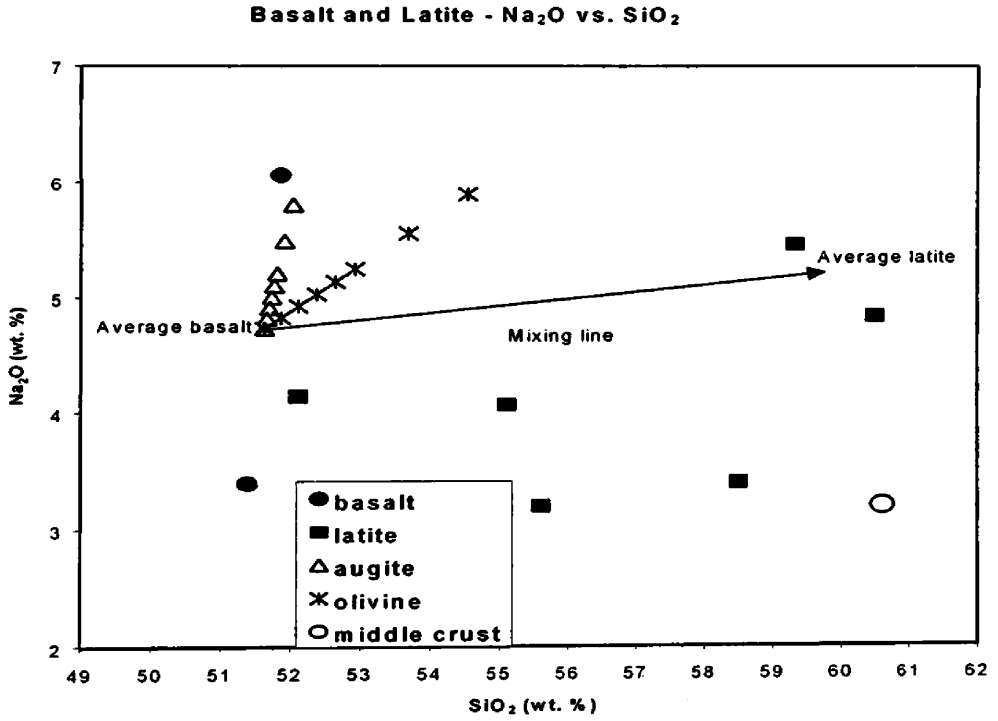

Figure 5h - Potential mixing of endmember basalt and latite. Incremental fractionation modeling of augite and olivine. See Figure 9 for a detailed explanation.

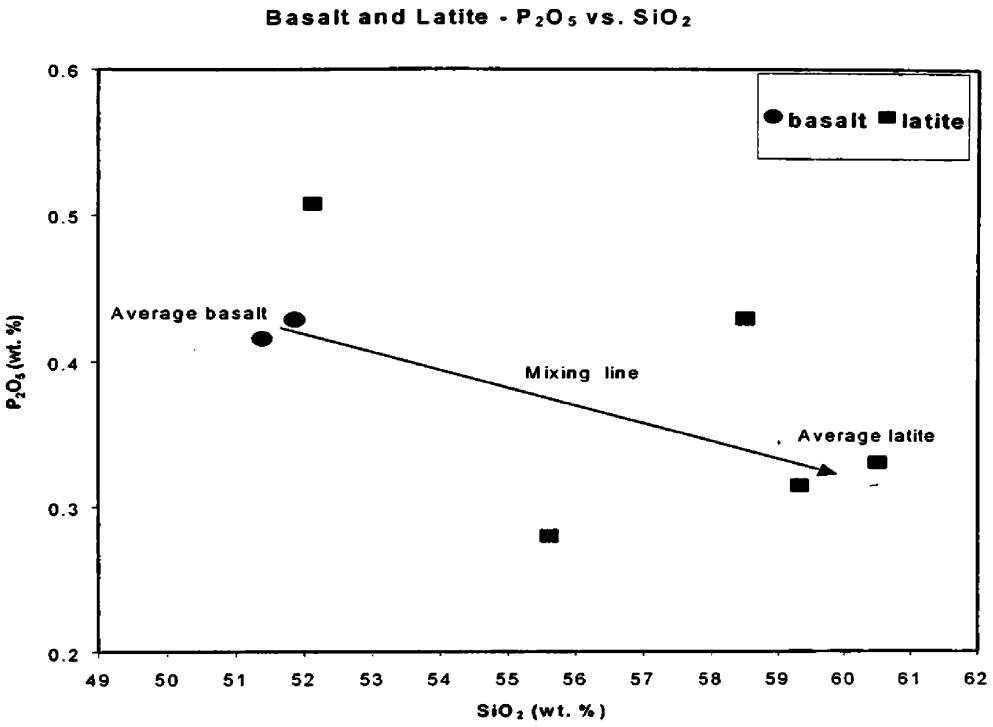

Figure 5i - Potential mixing of endmember basalt and latite.

Trace element partitioning is more sensitive to changes in magma composition than major elements and may provide more clues in unraveling petrogenic questions. Certain trace elements are preferentially partitioned into either the liquid or solid phase based primarily on the atomic radius and charge. Elements with a large distribution coefficient for a given mineral (i.e. greater than one) are partitioned preferentially into the crystalline phase and depleted in the remaining melt, and are considered compatible elements. The inverse, where elements are incompatible with the crystallizing phase, have distribution coefficients less than one as outlined in Appendix D. When a compatible element such as Cr or Ni is plotted with an incompatible element such as Rb, a straight line between end member magmas suggests that mixing has contributed to the generation of hybrid magmas. Figure 6 (a,b,c) show relevant trace element analysis. Significant scatter is evident which leads to the conclusion that mixing of basalt with latite was not the only process in producing intermediate compositions.

In other alkalic centers within Montana, latite is interpreted to form by melting of the lower to middle crust as the hot mafic magma ascends (Tureck-Schwartz 1992). As is demonstrated in Figure 5, for the most part, the composition of the average middle crust (Condie 1997, p. 61) does not fit within the latite field. This suggests that complete melting of the lower to middle crust to form latite was an insignificant part of the petrogenesis of the Adel Mountains volcanic rocks. However, partial melting of average middle crust would provide higher proportions of sodium, potassium, and probably aluminum (in feldspars), and lower proportions of magnesium and iron; the precise

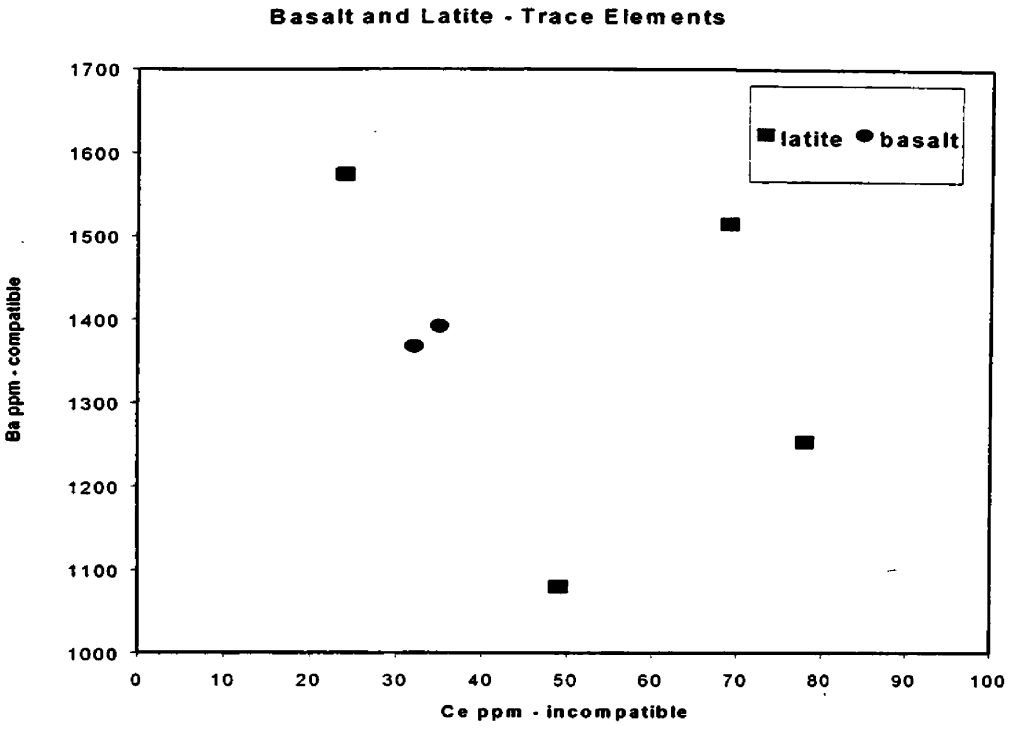

Figure 6a - Ba vs. Ce trace element plot of basalt and latite. A straight line correlation could suggest mixing as a possible source for intermediate rocks.

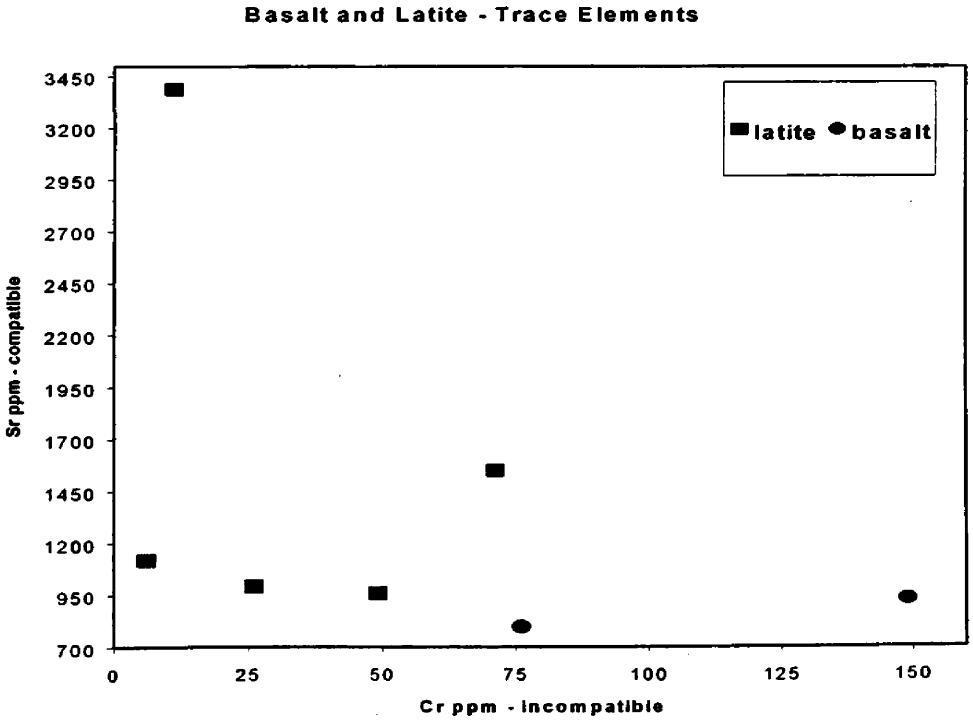

Figure 6b - Sr vs. Cr trace element plot of basalt and latite. A straight line correlation could suggest mixing as a possible source for intermediate rocks.

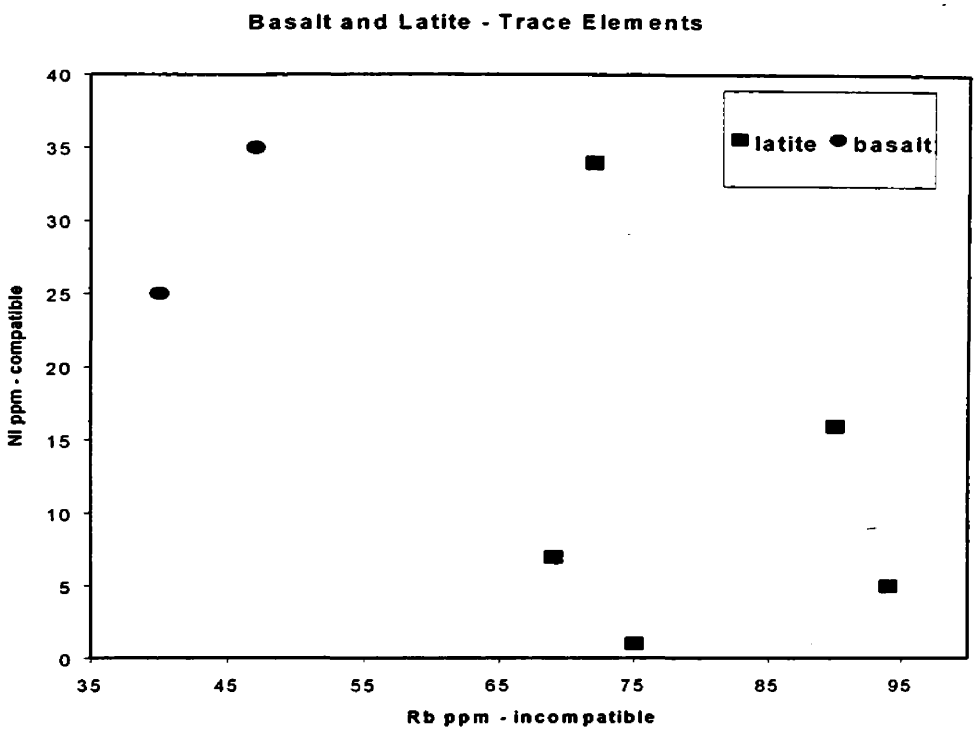

Figure 6c - Ni vs. Rb trace element plot of basalt and latite. A straight line correlation could suggest mixing as a possible source for intermediate rocks.

discrepancies seen between middle crust and the latite. Thus, partial melting of mid-crustal rocks to form end member latite is entirely viable.

Shonkinite as a Mafic Endmember for Mixing

In Figure 7 (a-i), the end of the mixing arrow is inferred as the parent shonkinite. In most cases, there appears to be a scattering of points which vaguely follow the trend expected between the end members. This type of general trend is best defined in Figure 7 e and h, which demonstrate a scattering along the defined mixing line. However, the reliability of CaO and Na_2O is variable since both tend to be mobile under certain conditions. The broad scatter in the other diagrams initially suggest that although magma mixing may have played a role in the generation of the Adel Mountains, other processes were more significant.

Further investigation utilizing trace elements supports the model of limited magma mixing between shonkinite and latite contributing to the petrogenesis of the Adel Mountains. Figure 8 (a,b,c) demonstrate considerable scatter without clear mixing patterns.

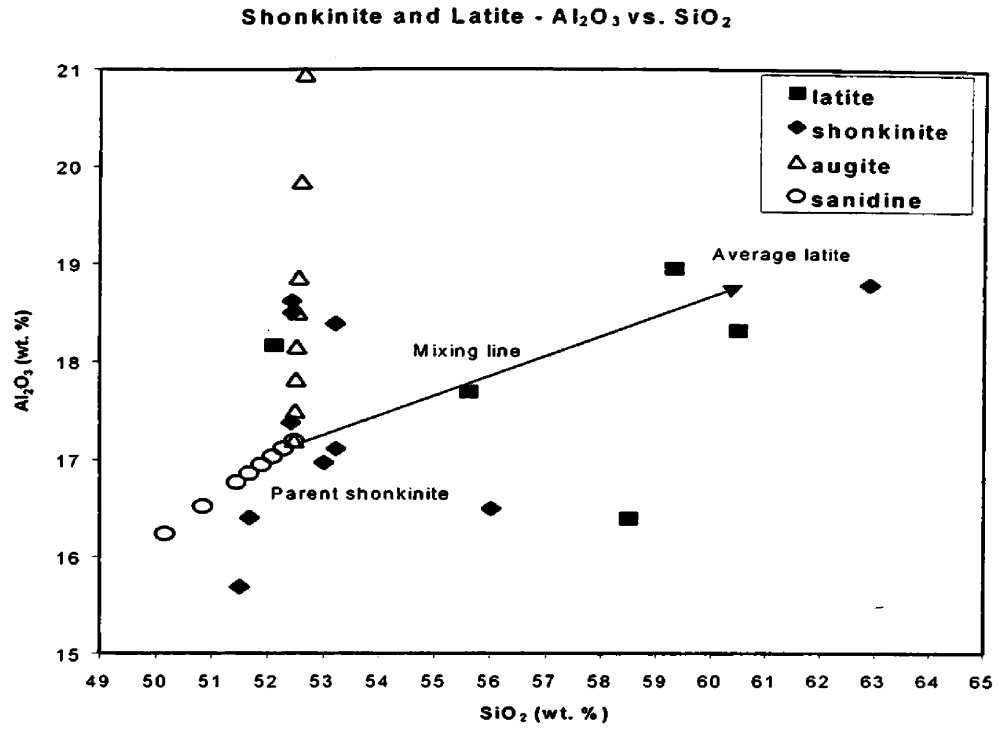

Figure 7a - Potential mixing of endmember shonkinite and latite. Incremental fractionation modeling of augite and sanidine from 0-20% phenocryst removal.

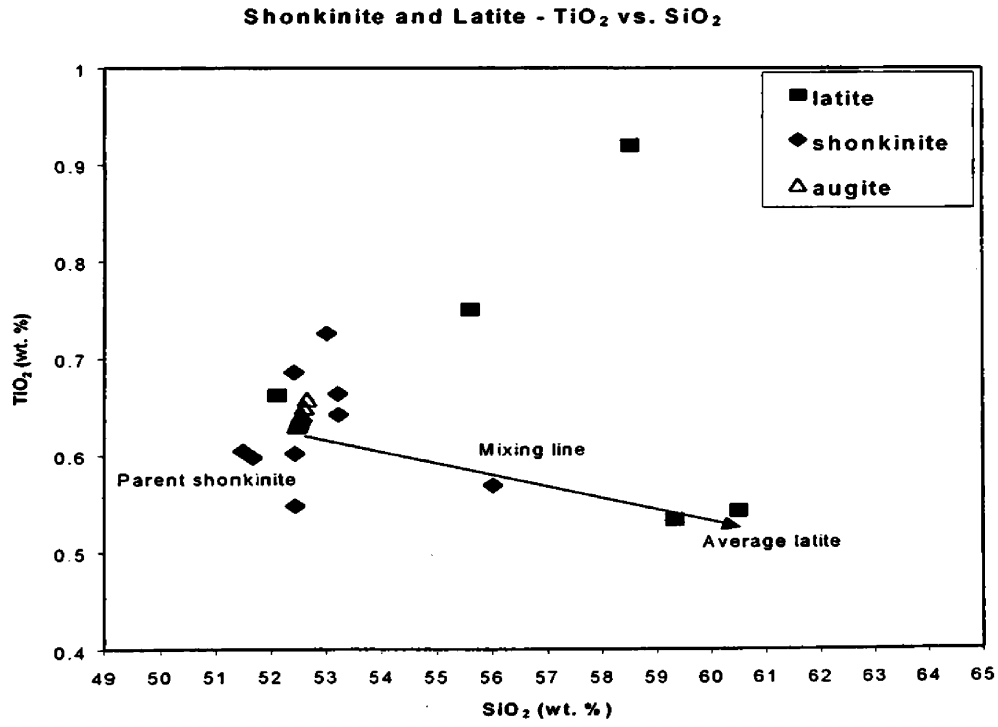

Figure 7b - Potential mixing of endmember shonkinite and latite. Incremental fractionation modeling of augite and sanidine from 0-20% phenocryst removal.

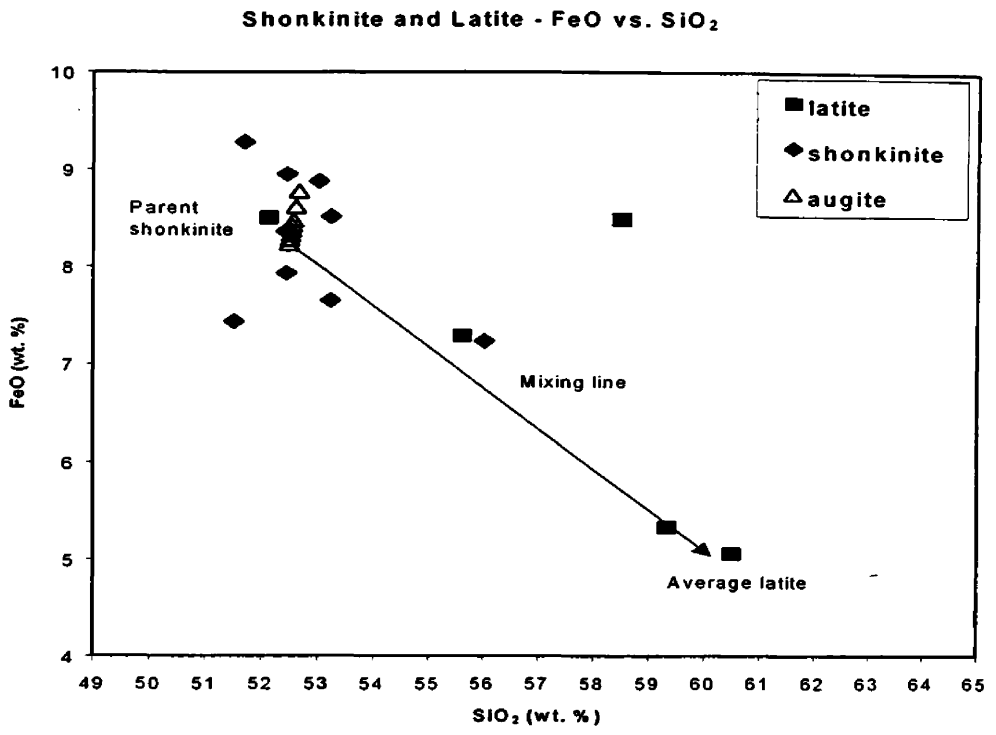

Figure 7c - Potential mixing of endmember shonkinite and latite. Incremental fractionation modeling of augite and sanidine from 0-20% phenocryst removal.

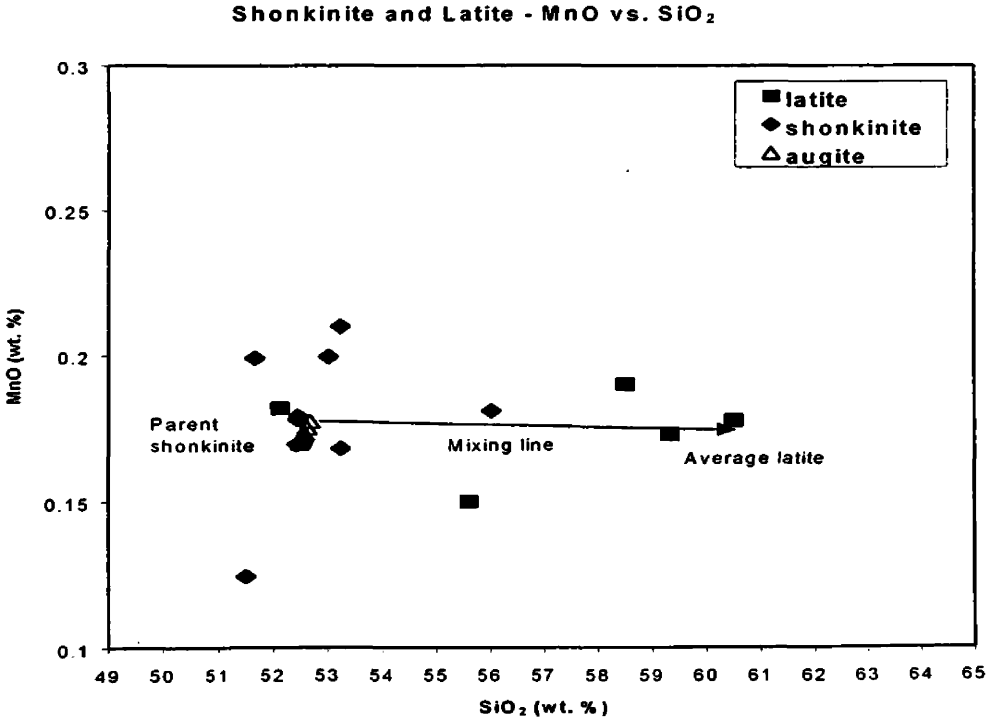

Figure 7d - Potential mixing of endmember shonkinite and latite. Incremental fractionation modeling of augite and sanidine from 0-20% phenocryst removal.

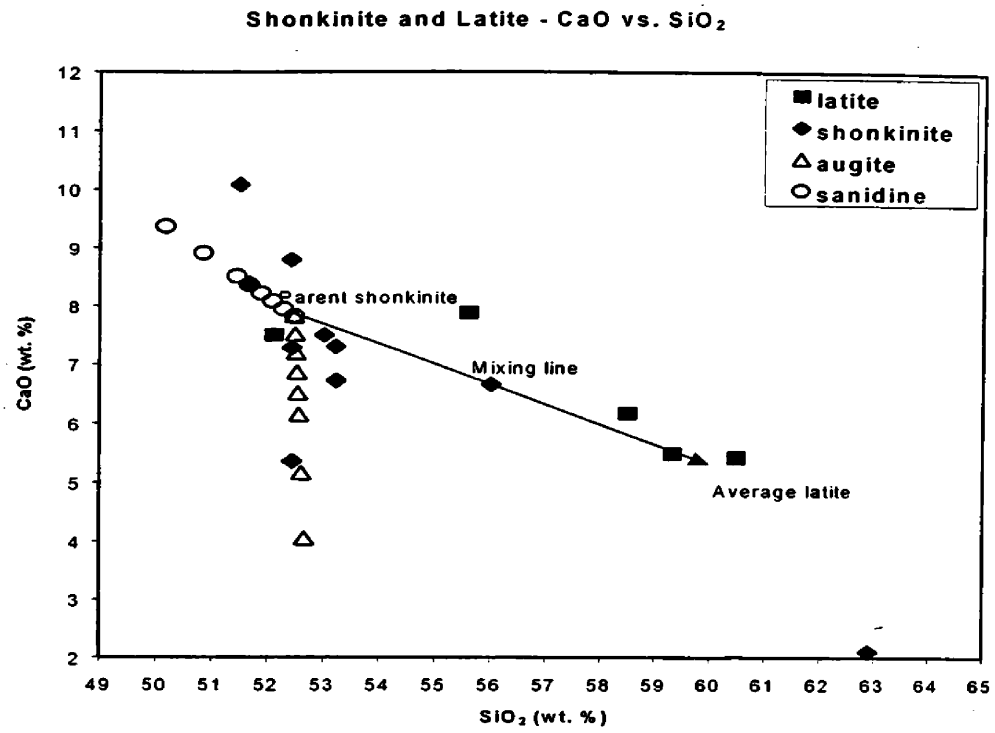

Figure 7e - Potential mixing of endmember shonkinite and latite. Incremental fractionation modeling of augite and sanidine from 0-20% phenocryst removal.

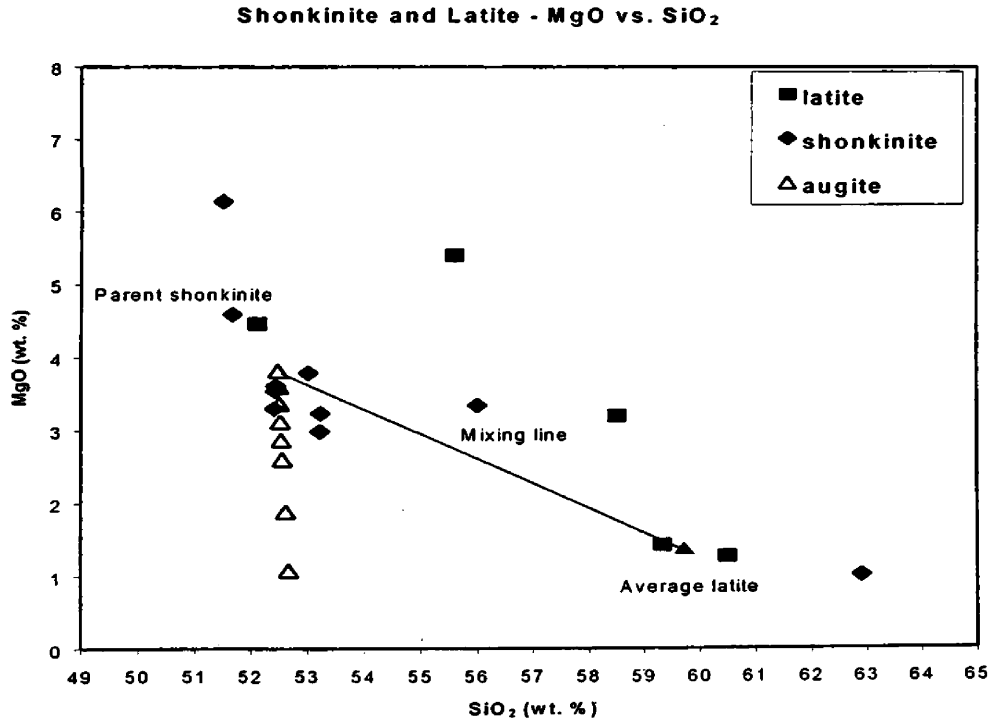

Figure 7f - Potential mixing of endmember shonkinite and latite. Incremental fractionation modeling of augite and sanidine from 0-20% phenocryst removal.

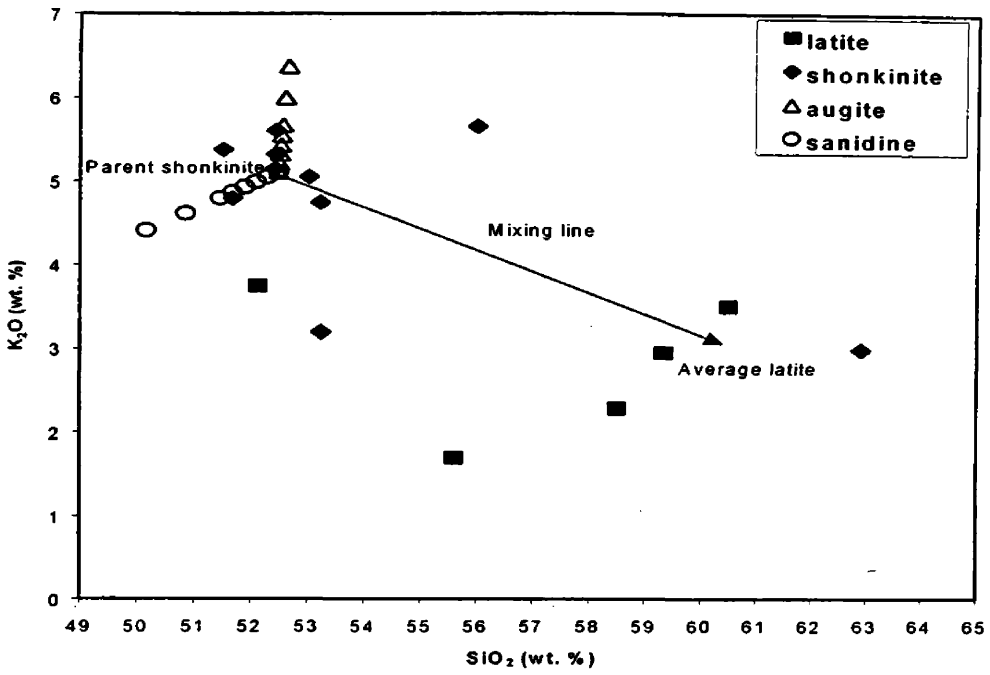

Figure 7g - Potential mixing of endmember shonkinite and latite. Incremental fractionation modeling of augite and sanidine from 0-20% phenocryst removal.

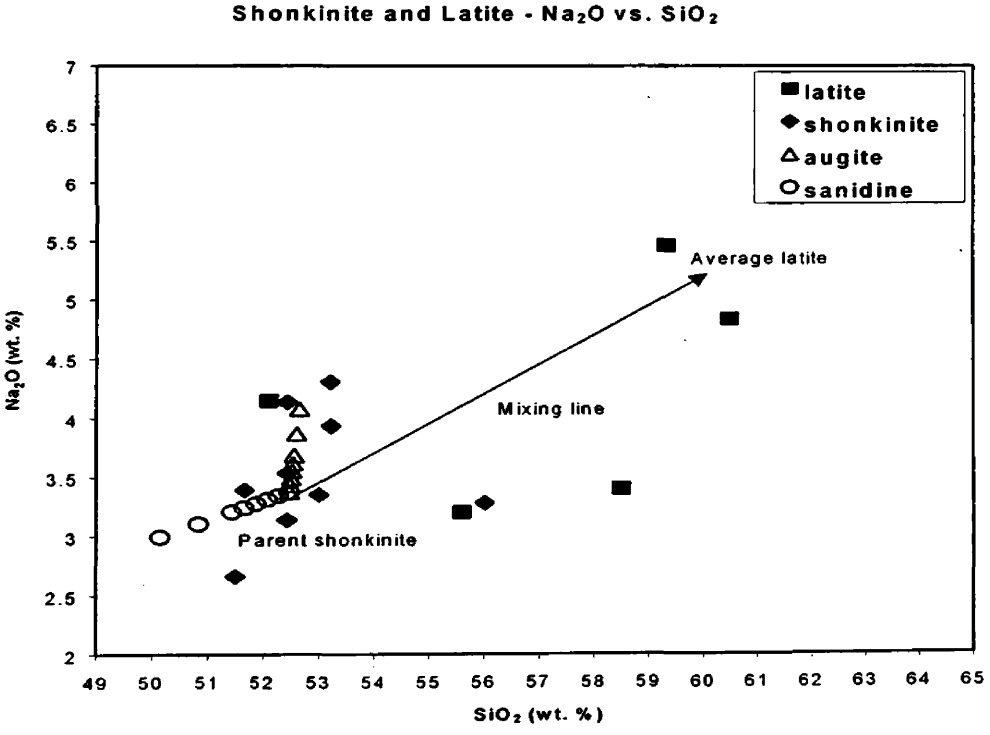

Figure 7h - Potential mixing of endmember shonkinite and latite. Incremental fractionation modeling of augite and sanidine from 0-20% phenocryst removal.

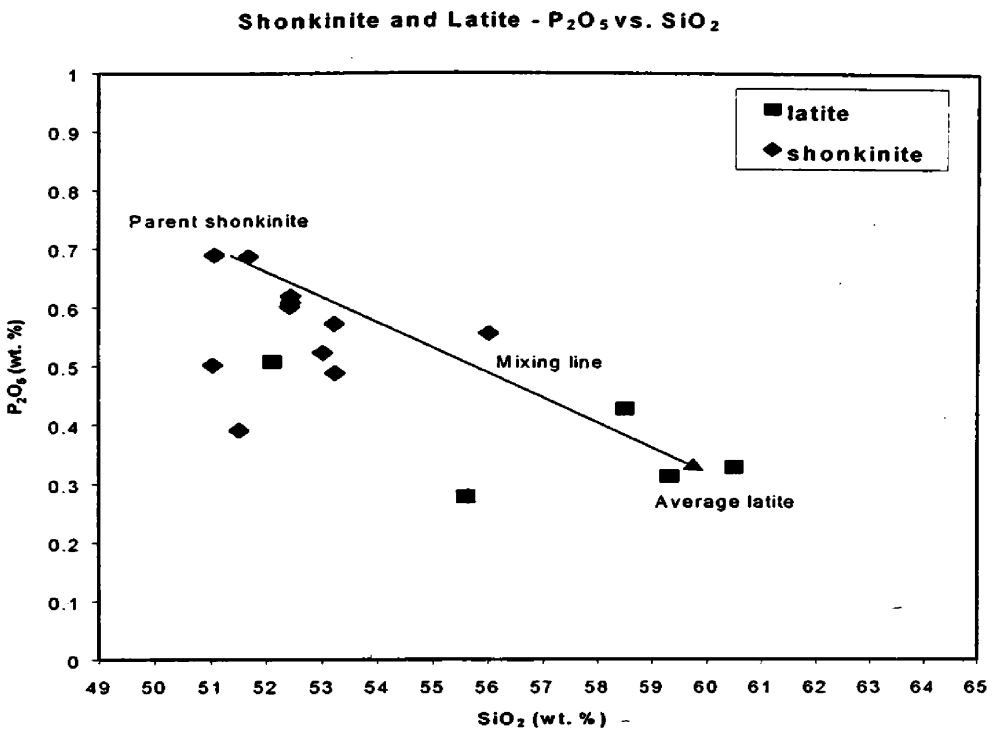

Figure 7i - Potential mixing of endmember shonkinite and latite. Incremental fractionation modeling of augite and sanidine from 0-20% phenocryst removal.

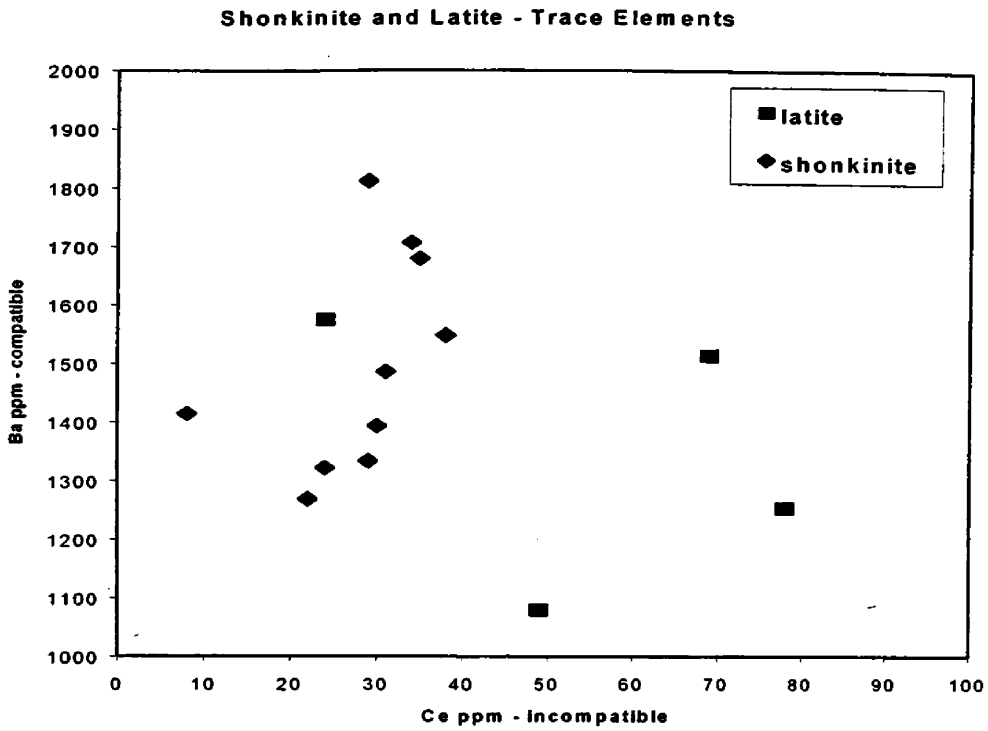

Figure 8a - Ba vs. Ce trace element plot of latite and shonkinite rocks. A straight line correlation could suggest mixing as a possible source for intermediate rocks.

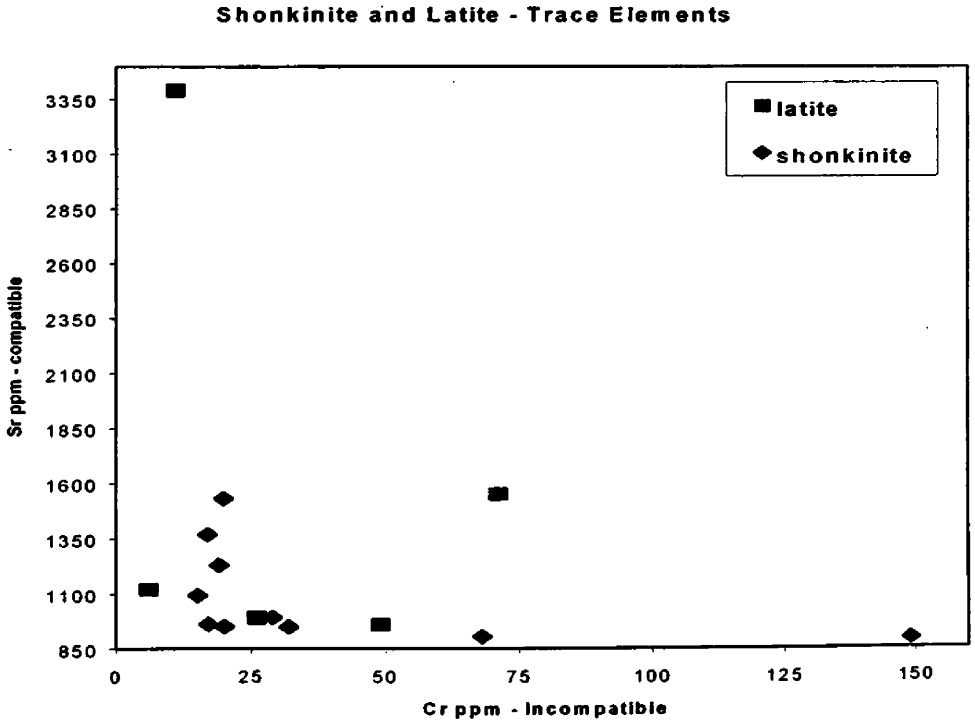

Figure 8b - Sr vs. Cr trace element plots of latite and shonkinite rocks. A straight line correlation could suggest mixing as a possible source for intermediate rocks.

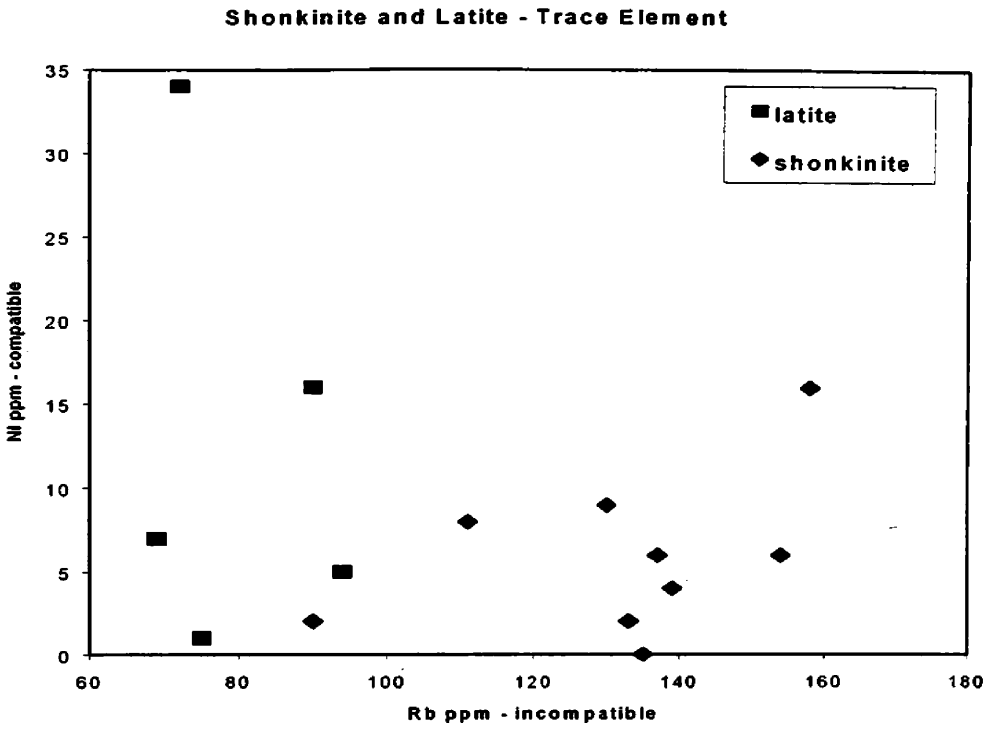

Figure 8c - Ni vs. Rb trace element plots of latite and shonkinite rocks. A straight line correlation could suggest mixing as a possible source for intermediate rocks.

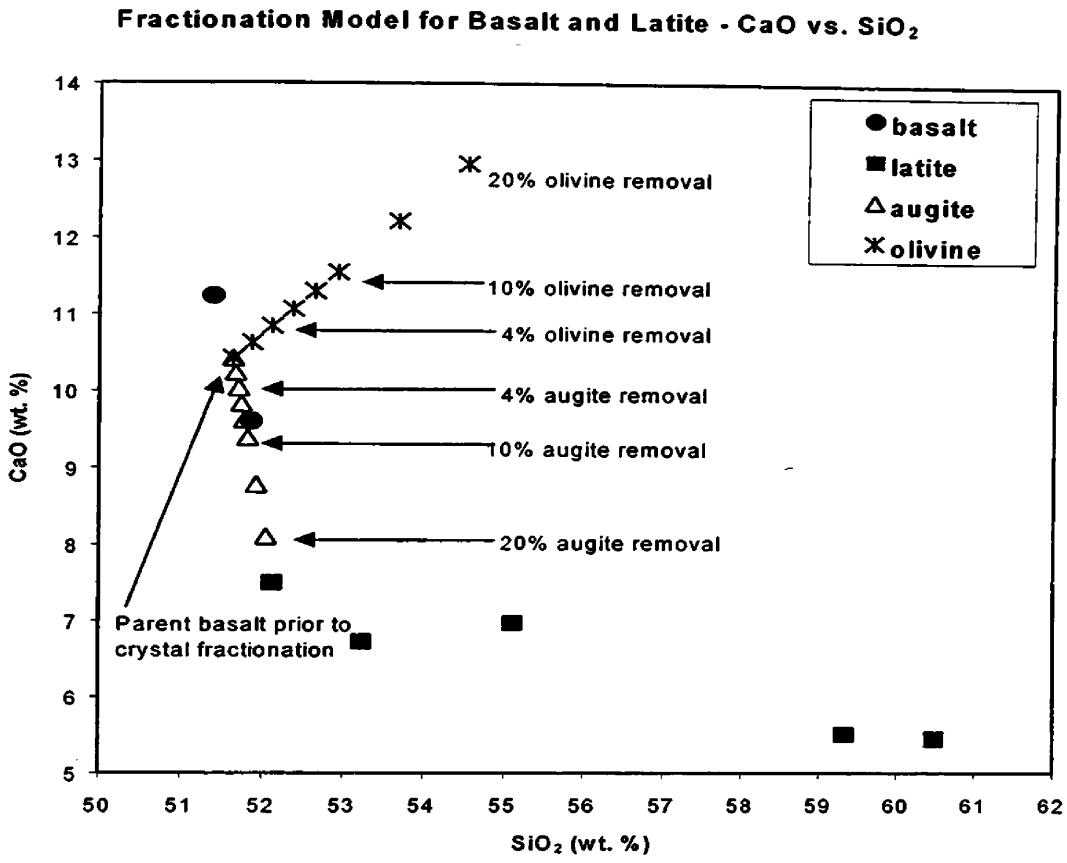

Figure 9 - Incremental fractionation model example. Mathematically calculated crystal removal for both augite and olivine in 2% increments from 0-10% then 5% increments from 10-20%. If basalt fractionates to form latite, the magma must proceed in a direction corresponding to the lines of incremental crystal removal. If proportions of olivine and augite are removed, the magma may follow along a vector between the end member crystal removal lines (i.e. augite and olivine). In the case shown here, crystallization of about 20% augite may have been followed by crystallization of augite and olivine together.

Chapter 5-3

GEOCHEMICAL MODELS FOR DIFFERENTIATION

Fractional Crystallization

Fractional crystallization represents the mechanical removal of a crystalline phase. Because each crystal accepts only certain elements into its mineral structure, both major and trace element geochemistry can provide insight into the crystallization history of fractionated magmas. By mathematically determining the composition of the remaining melt following modeled percentages of crystal removal, it is possible to infer the path a residual melt must take if crystal fraction is a primary process to form the latite. Modeling for the generation of latite from alkalic basalt and shonkinite melts is respectively discussed.

Alkalic Basalt as a Parent Melt

Figure 5 (a-i) demonstrate the necessary melt path for the removal of olivine, and augite with mineral analyses from Deer, Howie, and Zussman (1963). Analyses were chosen for a range of mineral compositions which might occur within the Adel Mountains. Specific references and values for the chosen minerals are available in Appendix E. Compositions of augite grains within the Adel Mountains were determined by microprobe and fall within the chemical variation between chosen Deer, Howie, and Zussman (1963) data as described above (Appendix F). Compositional variability is inherent in volcanic rocks and utilizing mineral ranges provides for representation of variation.

Appendix G provides the changing composition of the residual melt as 2-30% of both augite and olivine are fractionated. The melt path (and therefore, the increments of fractionation) should follow a trend directly away from the composition of the crystallizing phase if fractional crystallization has affected latite melts. Figure 9 illustrates the melt path if each phenocryst were removed individually. Removing proportions of both phenocryst phases would generate a vector between the end member augite removal line and the end member olivine removal line. Only minerals which project a melt path toward the latite can be significant fractionated phases.

Figure 5 (a-i) demonstrate that in order for latite to have formed as a result of fractional crystallization from basalt, augite must be the first phenocryst to crystallize and be removed. Further analysis suggests that a combination of augite and olivine may, in some cases, produce an appropriate melt curve which projects through some of the varying compositions of latite; this is compatible with the fractional crystallization model. Most likely, removal of labradorite was relatively minor in comparison to removal of augite and olivine. Since few plagioclase phenocrysts are present there is only a small Eu anomaly in the rare-earth element patterns. Eu removal is diagnostic of plagioclase fractionation (Figure 10).

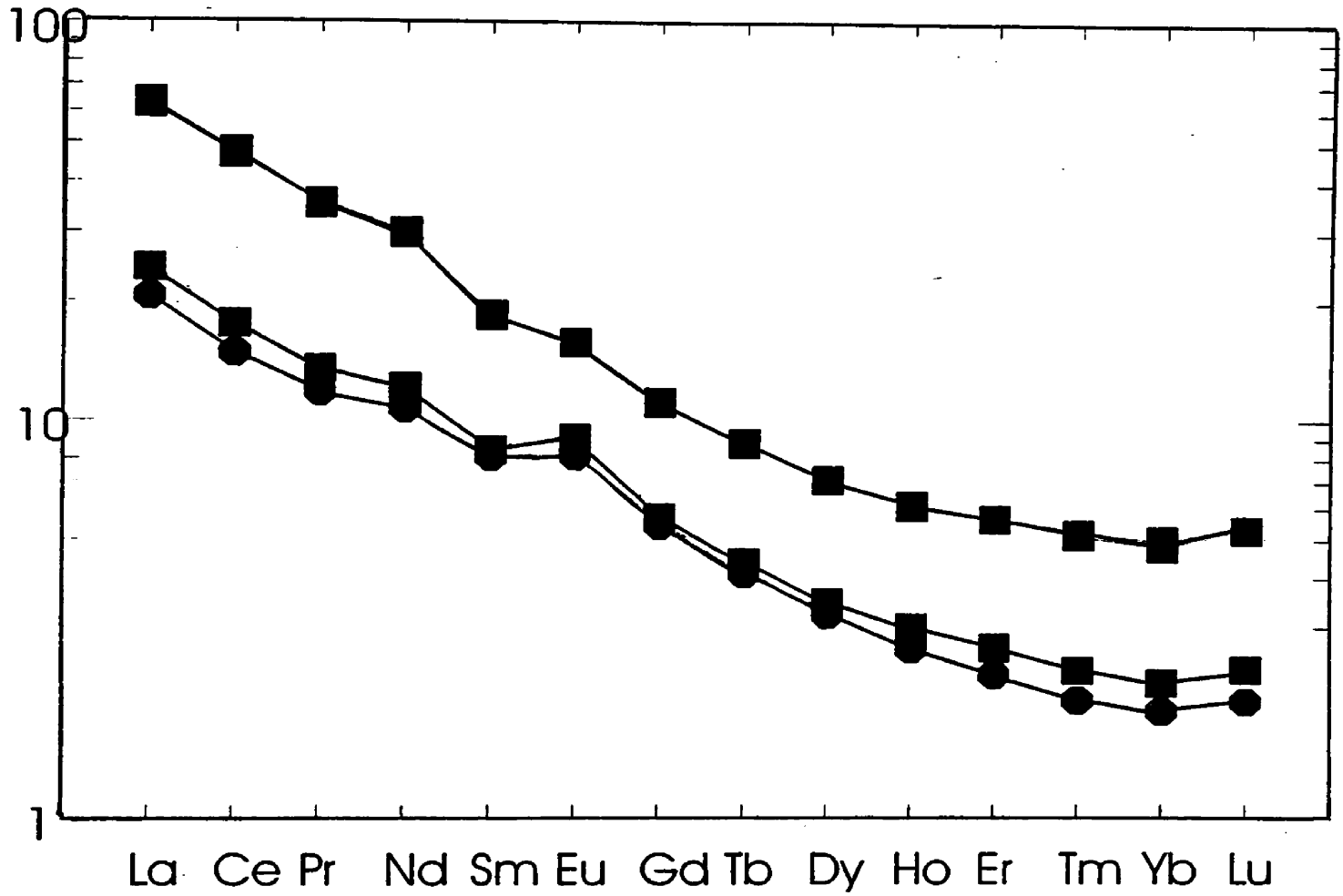

Figure 10 - Rare-earth element (REE) of basalt (circles) and latite (squares). Note the similarity between patterns for each of the rock types, thus suggesting a genetic relationship between the two.

However, many of the diagrams are not constrained to a single model and suggest that a combination of other processes played a significant role in the generation of latite. Figure 5 (a-e) demonstrate that a few of the latite samples may have evolved from a component of fractional crystallization while the others appear to result from mixing. The latite samples are somewhat divided by silica values. Samples with lower silica values (below 59% SiO_2) tend to have an origin compatible with a combination of fractional crystallization and mixing. The two latites with the highest silica values, as well as some intermediate compositions, may be the felsic mixing end member from partial melting of the middle crust as described in Chapter 5-2. A combination of mixing and fractional crystallization is compatible with the variation among the remaining latite samples.

Al_2O_3, FeO, CaO, and TiO_2 are the oxides which exhibit trends which are compatible with fractional crystallization. If this is a process which generates latite, why do we not see such constrained fractional crystallization curves in K_2O and Na_2O? These are relatively mobile. A plot of K_2O and Na_2O against another element such as thorium, which is detectable over a large range and generally considered immobile, provides a test of mobility. Figure 11 (a,b) show clearly that a wide range of compositions exist which supports sodium and potassium mobility. Compositions of samples from the Elkhorn Mountains are plotted for comparison. Rutland (1985) came to a similar conclusion in her analysis of the Elkhorn Mountains volcanic rocks.

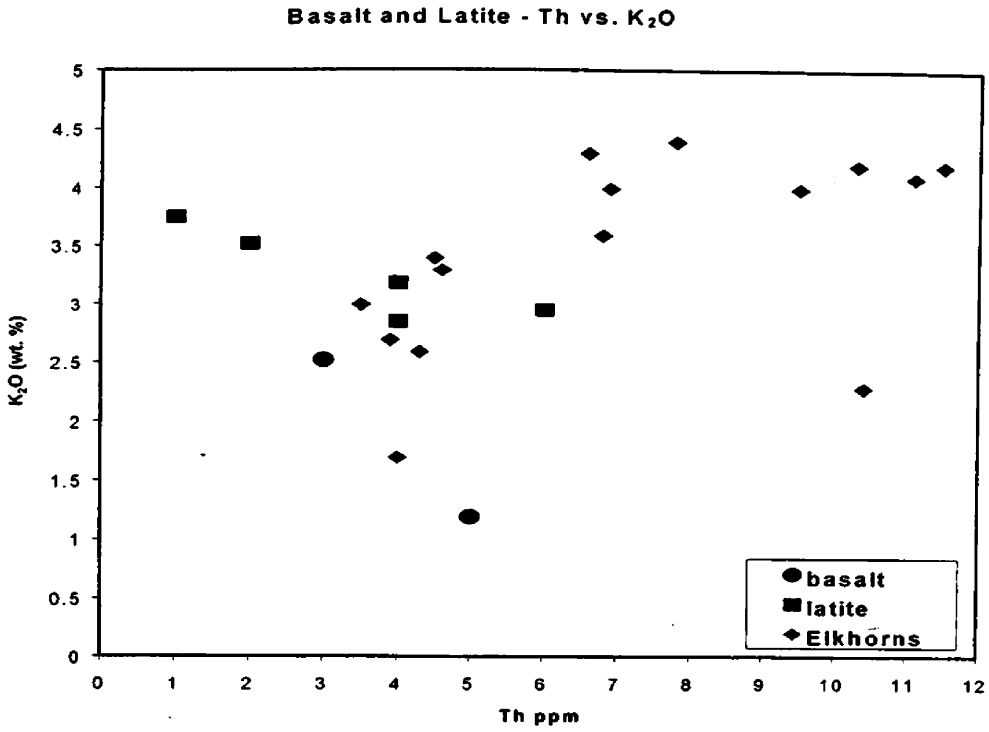

Figure 11a - K_2O vs. Th demonstrates the wide variation of K_2O compositions from the Adel Mountains which may suggest cation mobility. Elkhorns data (from Rutland 1985) are plotted for comparison.

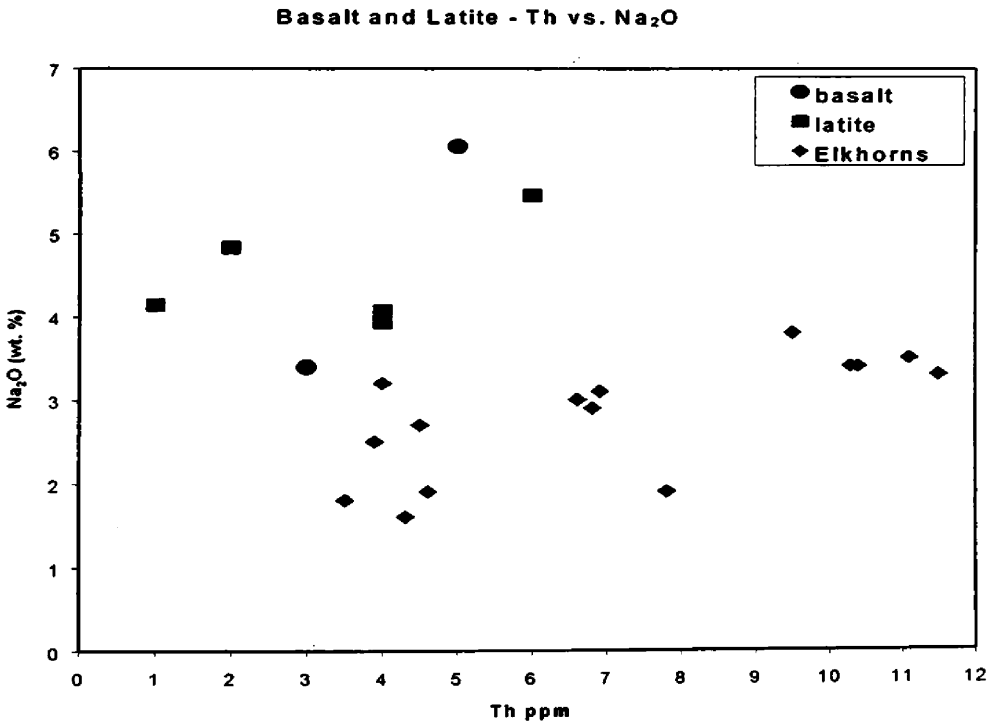

Figure 11b - Na_2O vs. Th demonstrates the wide variation in Na_2O compositions from the Adel Mountains which may suggest cation mobility. Elkhorns data (from Rutlan 1985) are plotted for comparison.

Further trace element evidence supporting the model that, in addition to mixing, some latite fractionated from basalt, includes concentrations of Ba, Rb, Zr, Nb, and Th since these elements are incompatible with most early crystallizing phases (Hyndman 1985 p. 116). When the felsic magma is enriched in these elements, it suggests that fractional crystallization, or partially melting of crustal rocks, may be a primary process in the generation of such magmas. With the exception of Th, each of the other elements show substantial enrichment in latite (Figure 12). Similarly, as is evident in Figure 10 a genetic relationship is apparent between rare-earth element concentrations (REE) in the basalt and latite.

Average concentrations in ppm

	Basalt	Latite
Ba	1381.0	1477.0
Rb	43.5	80.0
Zr	74.0	161.0
Nb	2.85	7.78
Th	4.0	3.4

Figure 12 - Concentrations of Ba, Rb, Zr, Nb, and Th in latite and basalt.

Shonkinite as a Parent Melt

Figure 7 (a-i) show Harker diagrams for the removal of augite and sanidine phenocrysts, and uses analyses from microprobe work by Tureck-Schwartz (1992) and Nash and Wilkinson (1970) (Appendix H). Although biotite and olivine are present as phenocryst phases in many classic shonkinites, the concentration of these minerals is minimal in the Adel Mountains. The chemistry of mineral phase compositions in the Bearpaw Mountains and Shonkin Sag laccolith samples are almost identical to the data obtained in

the Adel Mountains. The compositions of phenocryst phases that could possibly be fractionated are incrementally calculated from 0-30% (Appendix I). As with basalt, Figure 7 demonstrates the 0%-20% incremental removal of augite and sanidine from shonkinite. If fractionation were a primary process for the generation of the felsic rocks from shonkinite, latite would lie along the fractionation lines or along a vector between the two removed phenocryst phases. As is evident from the Figure 7 (a,e,f,g), the direction the residual magma must move from fractional crystallization is away from the latite trend. Latite data points are incompatible with fractional crystallization. With the combination of this test, field and petrographic evidence, I believe it is possible to rule out crystal fractionation from parent shonkinite as a major factor controlling variation in the Adel Mountains.

Liquid Immiscibility

Immiscibly separated magmas can be identified during field work. Generally, they form as globules or veinlets of one magma within another as is shown in Plate 7. Chemistry of the separated magmas can also be convincing. Mafic magmas that have been separated immiscibly are enriched in La and Ce (Watson 1976). Two samples (the syenite and mafic host from site shown in Plate 7) demonstrate the characteristic field relationships of the syenite forming felsic veinlets and globules within the shonkinite host and are plotted on a chondrite normalized spider diagram in Figure 13. The mafic rock is clearlyenriched in Ce. The two samples have similar normalized La concentration.

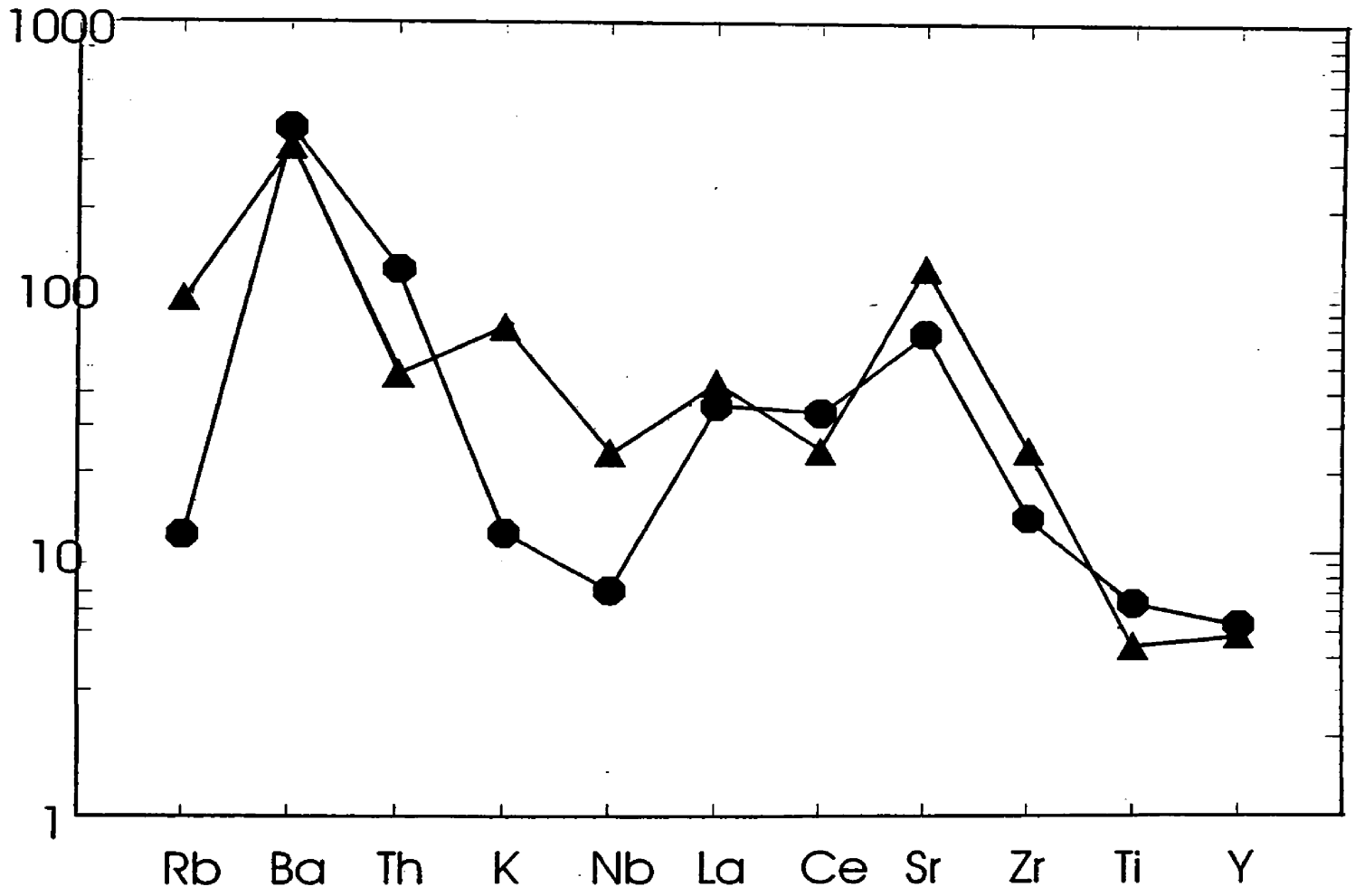

Figure 13 - Trace element plot of host mafic (circles) and syenite veinlets (triangles) normalized to chondrite values. Note that the mafic rock is more enriched in Ce than the syenite and the two rocks have overlapping La values which may suggest that they formed from liquid immiscibility.

Phosphorous concentrations are even more convincing. As discussed above, phosphorous and titanium generally concentrate in the mafic magma during liquid immiscible separation. Other processes concentrate these elements in the felsic phase. The average P_2O_5 percentage for shonkintes in the Adels is 0.576 while syenites average 0.408. The actual host of the syenite veinlets gives a P_2O_5 value of 0.429 while the syenite veinlets themselves have much lower values of 0.233. Titanium values give similar results (Figure 13). Average TiO_2 contents for host shonkinite are 0.632 while syenite values are only 0.541. Furthermore, the host of the syenite veinlets gives a high value of 0.697. Titanium and phosphorous concentrations along with field evidence and other chemical data, strongly suggest that liquid immisicibility is the primary process which formed the syenite veinlets.

Chapter 6

Discussion and Conclusion

The petrogenesis of the Adel Mountains is a complexly interwoven story involving a combination of magma mixing, crystal fractionation, liquid immiscibility, magma mingling, and generations of magmatic injections to form one of the more unique and less evolved eruptive centers of the central Montana Alkalic Province. A model compatible with the observed relationships involves a combination of processes, including;

1) End member latite formed from partial melting of mid-crustal rocks and was modified by mixing with a partially fractionated alkali basalt magma, as is evidenced by:

a) low Ni and Cr values of basalt which suggest it is not a primitive melt,

b) mixing models,

c) mid-crust partial melting models,

d) enrichment of the felsic rocks in Ba, Rb, Zr, and Nb,

2) Variation among some latite samples is compatible with some degree of fractional crystallization, as is evidenced by:

a) crystal fractionation diagrams,

b) zonation of augite grains in parent basalt,

c) enrichment of the felsic rocks in Ba, Rb, Zr, and Nb,

d) REE patterns which suggest a genetic relationship exists between basalt and latite,

3) Liquid immiscibility of a parent magma to form veinlets and globules of syenite in a shonkinite host,

a) high concentrations of P, Ti, La, and Ce in the mafic phase,

b) veinlets of syenite within host shonkinite in outcrop,

c) same mineral species in both the syenite veinlets and the shonkinite host,

4) Magma mingling between early and late stage shonkinte, basalt and shonkinite, and possibly latite and shonkinite,

a) mechanical interaction between the magmas - irregular dike borders, and truncated swirls as seen in outcrop,

b) distinct magmatic groups that cannot be co-genetic, i.e., shonkinite and basalt cannot form one from the other.

Beyond the immediate scope of the Adel Mountains, a crucial question remains; how can basalt and shonkinite be contemporaneous melts? Shonkinite is formed at depth by partial melting of a phlogopite-bearing phase to produce a high potassium melt (Hearn et. al. 1991). Basalt would form by partial melting of a lower potassic mantle. Shonkinite and basalt have also been observed to appear simultaneously in the nearby Elkhorn Mountains which where previously considered to be outside the area of the Alkalic Province. However, most samples of the Elkhorns are rather potassic as is evidenced by Figure 3 except for the few basalts which plot below the high potassium field. I propose

that the Elkhorn Mountains are part of the high potassium province and share sources similar to those of the Adel Mountains.

Although speculative, the edge of the Wyoming craton has previously been interpreted to lie near the southwestern boundary of the Adel Mountains. If the cratonic crust were to slope south (Figure 14), it seems reasonable to propose that the mantle may also slope southward from the boundary and therefore, the Adel Mountains. If the Wyoming craton marks the boundary between the edge of the anomalously alkalic mantle typically associated with the high potassium region of central Montana, it is reasonable to assume that partial melting of such a high potassium mantle would produce shonkinitic melts. Beyond the area of the high potassium mantle, less potassic melts would generate basalt. If the mantle follows the sloping cratonic boundary, the model would generate less shonkinite farther south while more potassic magmas would be found to the north of the boundary.

As is evidenced by previous studies, the Boulder batholith becomes more sodic toward its southern border while the northern edge remains more potassic (Tilling 1973). Similarly, the Elkhorn Mountains, northeast of the Boulder batholith, also demonstrate a significant proportion of potassium bearing. As is outlined in Figure 14, I suggest that the combination of basalt and shonkinite may be related to partial melting of different proportions of either potassic, or less alkalic mantle as it slopes beneath the border of the Wyoming craton. With this model, it is possible to generate both alkaline and alkaline rocks simultaneously.

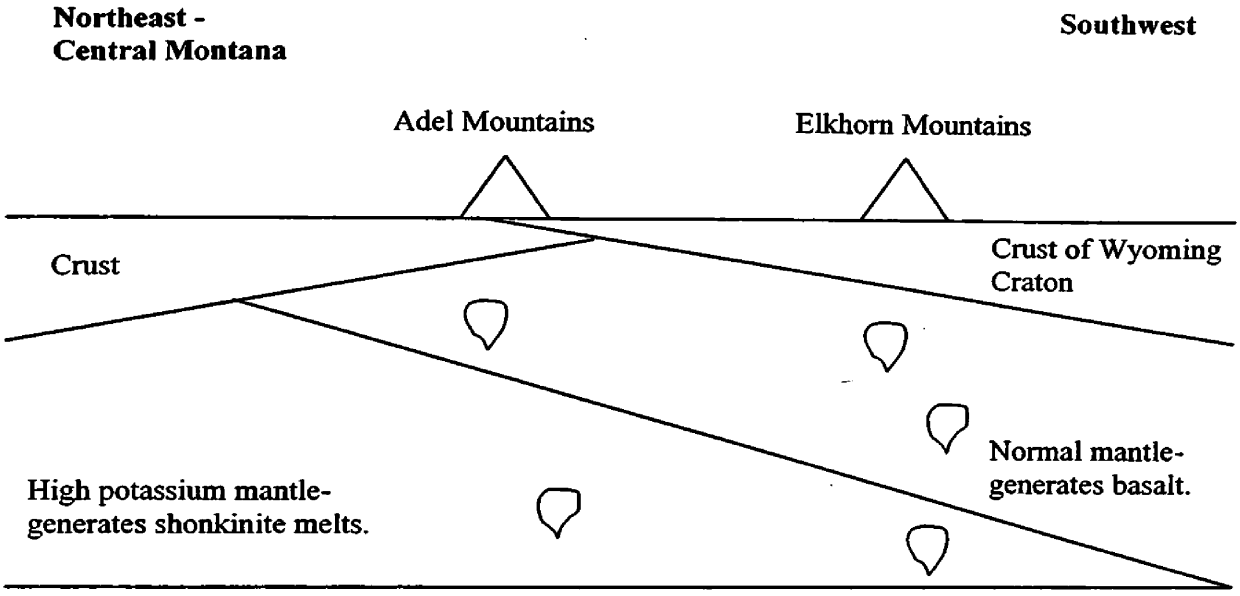

Figure 14 - Schematic sketch of proposed model. The slope of the Wyoming craton is mimicked by the mantle where partial melting results in basalt generation. To the northeast, the alkaline mantle beneath central Montana contributes high potassium magma during partial melting. This scenario enables both alkalic melts (shonkinite) and non-alkalic melts (basalt) to be generated simultaneously in the same location.

Appendices A-I

APPENDIX A - XRF data for the Adel Mountains

Sample No.	Rock Type	SiO2	TiO2	MgO	Al2O3	FeO	MnO	CaO	K2O	Na2O
6-26-9	basalt	51.39	0.641	6.39	16.09	7.78	0.139	11.24	2.52	3.39
6-27-1	basalt	51.86	0.697	4.69	16.96	8.38	0.138	9.60	1.20	6.06
7-6-1	latite	59.32	0.533	1.42	18.97	5.34	0.173	5.51	2.96	5.46
7-6-2	latite	60.49	0.542	1.27	18.33	5.06	0.177	5.45	3.52	4.83
7-6-3	latite	52.12	0.662	4.46	18.16	8.51	0.182	7.51	3.74	4.15
9-12-2	latite	55.11	0.569	1.49	18.85	5.59	0.168	6.98	2.86	4.07
9-12-8	latite	53.23	0.642	3.23	17.11	8.52	0.210	6.73	3.19	3.93
45*	latite	62.90	0.300	1.00	18.80			2.10	3.00	7.40
6-26-10	shonkinite	51.51	0.604	6.14	15.69	7.44	0.124	10.08	5.38	2.66
7-5-1	shonkinite	53.01	0.726	3.79	16.97	8.88	0.200	7.51	5.05	3.35
6-26-2	shonkinite	52.44	0.602	3.62	18.50	8.95	0.179	5.36	5.60	4.13
6-26-3	shonkinite	52.44	0.548	3.54	18.62	7.93	0.178	7.29	5.32	3.53
6-26-4	shonkinite	52.42	0.685	3.30	17.38	8.37	0.170	8.80	5.15	3.13
6-26-5	shonkinite	51.68	0.598	4.59	16.40	9.28	0.199	8.39	4.79	3.39
6-26-6	shonkinite	56.01	0.568	3.34	16.50	7.25	0.181	6.68	5.65	3.28
7-7-2	shonkinite	53.22	0.663	2.98	18.39	7.66	0.168	7.30	4.75	4.30
9-12-3	shonkinite	51.06	0.671	3.96	16.19	8.41	0.184	7.97	5.18	3.06
9-12-7	shonkinite	51.03	0.650	2.93	17.26	8.26	0.145	8.90	4.24	2.91
78*	shonkinite	52.50	0.70	4.30	17.00			7.40	4.10	3.20
92a*	shonkinite	51.30	0.60	4.30	16.00			7.70	5.60	3.40
91*	shonkinite	51.10	0.60	4.50	17.30			7.10	5.20	3.10
019*	shonkinite	51.20	0.70	4.60	17.20			7.70	4.10	2.80
93*	shonkinite	51.60	0.60	5.90	16.50			5.50	5.80	2.90
46*	shonkinite	54.30	0.50	2.80	17.80			6.90	5.10	3.20
49*	shonkinite	56.70	0.40	0.90	19.60			4.80	5.70	5.80
47*	shonkinite	58.10	0.50	1.50	20.00			3.70	4.40	4.90
90b*	shonkinite	62.80	0.20	0.90	18.20			4.80	4.10	4.10
7-7-1	syenite	53.86	0.663	3.37	17.59	7.80	0.174	6.92	6.08	2.96
6-27-2	syenite	53.60	0.481	1.39	21.80	4.45	0.089	7.92	7.29	2.76
035*	syenite	51.90	0.60	3.70	16.90			6.80	6.10	3.00

* = Values from Beall (1973) p. 75.

Sample No.	Rock Type	P2O5	Ni	Cr	Sc	V	Ba	Rb	Sr	Zr
6-26-9	basalt	0.416	35	149	36	189	1393	47	929	74
6-27-1	basalt	0.429	25	76	29	207	1369	40	796	74
7-6-1	latite	0.315	34	71	11	58	1516	72	1548	193
7-6-2	latite	0.331	5	11	12	54	1960	94	3390	250
7-6-3	latite	0.508	16	49	22	205	1575	90	958	81
9-12-2	latite	0.361	1	6	16	64	1255	75	1119	179
9-12-8	latite	0.489	7	26	23	202	1080	69	992	102
45*	latite									
6-26-10	shonkinite	0.391	31	149	27	164	1322	182	893	71
7-5-1	shonkinite	0.523	0	20	23	201	1394	135	950	89
6-26-2	shonkinite	0.62	16	68	11	175	1812	158	904	89
6-26-3	shonkinite	0.61	9	20	20	164	1680	130	1531	116
6-26-4	shonkinite	0.60	2	17	21	170	1269	133	1368	108
6-26-5	shonkinite	0.69	6	32	22	187	1549	137	948	91
6-26-6	shonkinite	0.558	6	17	16	141	1487	154	961	106
7-7-2	shonkinite	0.573	4	19	21	170	1334	139	1229	103
9-12-3	shonkinite	0.689	8	29	20	189	1707	111	992	98
9-12-7	shonkinite	0.502	2	15	21	173	1414	90	1092	100
78*	shonkinite									
92a*	shonkinite									
91*	shonkinite									
019*	shonkinite									
93*	shonkinite									
46*	shonkinite									
49*	shonkinite									
47*	shonkinite									
90b*	shonkinite									
7-7-1	syenite	0.583	5	23	20	179	2301	194	1030	95
6-27-2	syenite	0.233	2	6	11	65	1173	317	1425	134
035*	syenite									

* = Values from Beall (1973) p. 75.

Sample No.	Rock Type	Y	Nb	Ga	Cu	Zn	Pb	La	Ce	Th
6-26-9	basalt	10	3.1	15	57	65	10	12	35	3
6-27-1	basalt	12	2.6	15	59	71	5	13	32	5
7-6-1	latite	24	9.4	23	0	112	13	39	69	6
7-6-2	latite	22	8.4	18	0	110	15	42	77	2
7-6-3	latite	11	4.1	21	53	80	11	10	24	1
9-12-2	latite	25	11.5	27	0	123	25	42	78	4
9-12-8	latite	16	5.5	19	24	98	15	36	49	4
45*	latite									
6-26-10	shonkinite	12	3.4	16	42	60	13	2	24	0
7-5-1	shonkinite	15	4.1	22	25	113	10	10	30	3
6-26-2	shonkinite	13	5.9	16	67	92	15	18	29	4
6-26-3	shonkinite	15	4.5	19	48	86	19	28	35	3
6-26-4	shonkinite	17	5.5	23	31	96	13	6	22	4
6-26-5	shonkinite	13	6.4	19	66	89	17	5	38	3
6-26-6	shonkinite	16	5.2	16	36	87	15	33	31	2
7-7-2	shonkinite	15	5.2	19	32	93	15	27	29	5
9-12-3	shonkinite	15	7.0	18	71	89	15	7	34	6
9-12-7	shonkinite	15	5.2	18	24	86	14	15	8	4
78*	shonkinite									
92a*	shonkinite									
91*	shonkinite									
019*	shonkinite									
93*	shonkinite									
46*	shonkinite									
49*	shonkinite									
47*	shonkinite									
90b*	shonkinite									
7-7-1	syenite	16	5.0	15	37	94	13	16	27	1
6-27-2	syenite	11	8.8	26	7	59	14	16	23	2
035*	syenite									

* = Values from Beall (1973) p. 75.

APPENDIX B - Discussion of XRF preparation methods and accuracy

Sample preparation for XRF analyses from Johnson et. al. (in press).

Fresh chips of the sample are hand picked and a standard volume of chips (28 grams) are ground in a swing mill with tungsten carbide surfaces for 2 minutes. 3.5 grams of the sample powder is weighed into a plastic mixing jar with 7.0 grams of spec pure dilithium tetraborate and, assisted by an enclosed plastic ball, mixed for ten minutes. The mixed powders are emptied into graphite crucibles with internal measurements of 34.9 mm diameter by 31.8 mm deep. 24 filled crucibles are placed on a silica tray and loaded into a muffle furnace only large enough to contain the tray. Fusion takes 5 minutes from the time the preheated furnace returns to its normal 1000 decree Celcius after loading. The silica plate and graphite crucibles are then removed from the oven and allowed to cool. Each bead is reground in the swing mill for 35 seconds, the glass powder then replaced in the graphite crucibles and refused for 5 minutes.

Following the second fusion, the cooled beads are labeled with an engraver, their lower flat surface is ground on 600 silicon carbide grit, finished briefly on a glass plate to remove any metal from the grinding wheels, washed in an ultrasonic cleaner, rinsed in alcohol and wiped dry. The glass beads are then ready to be loaded into the XRF spectromemter. Preparation of a single bead takes 45 minutes.

Precision

Two standard beads are used as internal standards. Kept in the same position in the automatic loader, they run between every 28 unknown samples and so provide a continuing check on instrumental performance.

Accuracy

The WSU GeoAnalytical Lab estimates the accuracy of analyses in two ways: 1) by the scatter of the standard samples around the calibration curve for each element; 2) and by comparing these values to those of the same samples analyzed by other workers in different laboratories and using different techniques.

Johnson, D.M., Hooper, P.R., and Conrey, R.M., *XRF analysis of rocks and minerals for major and trace elements on a single low dilution Li-tetraborate fused bead*, Advances in X-Ray Analysis, 41, in press.

APPENDIX C - L.O.I., MgO, Na_2O values for "average" determinations

Sample	L.O.I	MgO	Na2O
6-26-10	7.36	6.14	2.66
7-5-1	3.88	3.79	3.35
6-26-2	5.17	3.62	4.13
6-26-3	4.75	3.54	3.53
6-26-4	4.11	3.30	3.13
6-26-5**	4.04	4.59	3.39
6-26-6	3.70	3.34	3.28
7-7-2	4.73	2.98	4.3
9-12-3**		3.96	3.06
9-12-7		2.93	2.91
7-6-1**	2.04	1.42	5.46
7-6-2	5.51	1.27	4.83
7-6-3	5.05	4.46	4.15
9-12-2**		1.49	4.07
9-12-8		3.23	3.93

** = Samples used to determine rock averages.

APPENDIX D - Kd values for trace element analysis

	K	Rb	Sr	Ba
Mafic CPX	0.002-0.1	0.001-0.07	0.067-0.25	0.001-0.08
Mafic Plagioclase	0.1-0.3	0.05-0.2	0.3-2.2	0.14-0.5
Felsic Kspar	0.037	0.032	0.516	0.131
	La	Ce	Ni	Cr
Mafic CPX	0.026-0.25	0.1-0.25	0.5-4.4	0.03-13
Mafic Plagioclase	0.02-0.3	0.1	0.01-0.06	0.01-0.02
Felsic Kspar		0.5		

Data from Hyndman 1985.

APPENDIX E - Basalt probe values from Deer, Howie, and Zussman (1963)

Basalt Microprobe Values and References

Labradorite			Augite			Olivine		
	#12 - A	#10 - B		#5 - A	#11 - B		#6-A	#8-B
SiO2	52.33	52.97	SiO2	48.11	51.86	SiO2	40.84	39.12
TiO2			TiO2	1.14	0.55	TiO2	0.04	0.09
Al2O3	30.22	29.41	Al2O3	7.26	2.33	Al2O3	0.19	0.58
FeO			FeO	4.86	9.45	FeO	8.18	10.76
MgO			MnO	0.11	0.24	MnO	0.17	0.16
CaO	12.52	12.59	MgO	14.04	14.5	MgO	50.27	46.51
Na2O	3.62	3.97	Cao	20.46	18.92	Cao	0	0.48
K2O	0.85	0.26	Na2O	0.66	0.23	Na2O	0	0.15
			K2O	0.04	0	K2O	0	0.06

Labradorite - A = Hutchinson and Campbell Smith, 1912
Labradorite - B = Larsen and Draisin, 1948
Augite - A = Aoki, 1959
Augite - B = Hess, 1949
Olivine - A = Hawkes, 1946
Olivine -B = Mathias, 1949
from Deer, Howie, and Zussman, 1963, Rock Forming Minerals,
NY: John Wiley and Sons, Inc., vol. 1, 2,4.

APPENDIX F - Adel Mountains probe data

Sample	Na2O	Al2O3	SiO2	Fe2O3	K2O	CaO	MgO	MnO	TiO2	Cr2O3	SUM
6-26-05											
augite	0.51	3.56	50.50	9.12	0.01	22.45	13.97	0.38	0.54	0.00	101.04
core	0.42	3.95	50.37	9.26	0.01	22.63	13.53	0.33	0.54	0.00	101.04
rim	0.58	4.24	49.75	9.71	0.00	22.01	13.12	0.37	0.63	0.02	100.42
middle	0.41	3.15	50.85	9.21	0.00	22.39	13.88	0.31	0.44	0.02	100.65
augite											
core	0.49	3.71	50.68	9.44	0.00	22.10	13.29	0.29	0.48	0.00	100.50
rim	0.51	4.11	49.63	9.60	0.00	21.81	13.37	0.34	0.60	0.02	99.98
6-26-9											
augite core	0.35	4.99	48.98	8.64	0.00	22.72	13.50	0.17	0.69	0.01	100.06
outward	0.35	4.44	49.36	9.38	0.01	22.50	13.52	0.18	0.70	0.01	100.45
outward	0.21	2.47	52.33	5.93	0.00	23.33	15.73	0.15	0.26	0.03	100.45
rim	0.45	3.87	49.76	9.76	0.01	22.13	13.44	0.19	0.72	0.00	100.34
augite											
core	0.27	2.53	52.20	4.57	0.00	23.42	16.51	0.05	0.26	0.27	100.08
rim	0.49	5.10	48.15	9.94	0.01	22.29	12.68	0.18	0.98	0.00	99.82
augite											
core	0.25	2.85	51.33	5.13	0.01	23.25	16.20	0.04	0.30	0.12	99.47
outward	0.44	5.45	47.80	10.00	0.01	22.51	12.67	0.22	1.02	0.03	100.15
rim	0.40	5.60	46.94	9.56	0.04	22.74	12.53	0.21	1.08	0.03	99.12

APPENDIX G - Incremental calculations for fractional crystallization from alkalic basalt

	SiO2	TiO2	MgO	Al2O3	FeO	MnO	CaO	K2O	Na2O
Average basalt comp	51.63	0.67	5.54	16.52	8.08	0.14	10.42	1.86	4.73
Average augite comp	49.99	0.845	14.27	4.8	7.16	0.175	19.69	0.02	0.445
Average olivine comp	39.98	0.065	48.39	0.385	9.47	0.165	0.24	0.03	0.075
Augite									
% crystals removed									
0	51.63	0.670	5.54	16.52	8.08	0.140	10.42	1.86	4.73
2	51.66	0.666	5.36	16.76	8.10	0.139	10.23	1.90	4.82
4	51.70	0.663	5.18	17.01	8.12	0.139	10.03	1.94	4.91
6	51.73	0.659	4.98	17.27	8.14	0.138	9.83	1.98	5.00
8	51.77	0.655	4.78	17.54	8.16	0.137	9.61	2.02	5.10
10	51.81	0.651	4.57	17.82	8.18	0.136	9.39	2.06	5.21
15	51.92	0.639	4.00	18.59	8.24	0.134	8.78	2.18	5.49
20	52.04	0.626	3.36	19.45	8.31	0.131	8.10	2.32	5.80
30	52.33	0.595	1.80	21.54	8.47	0.125	6.45	2.65	6.57
Olivine									
% crystals removed									
0	51.63	0.670	5.54	16.52	8.08	0.140	10.42	1.86	4.73
2	51.87	0.682	4.67	16.85	8.05	0.139	10.63	1.89	4.83
4	52.12	0.695	3.75	17.19	8.02	0.139	10.84	1.93	4.92
6	52.37	0.709	2.80	17.55	7.99	0.138	11.07	1.96	5.03
8	52.64	0.723	1.81	17.92	7.96	0.138	11.31	2.00	5.13
10	52.92	0.737	0.78	18.31	7.93	0.137	11.55	2.04	5.25
15	53.69	0.777	-2.02	19.37	7.83	0.136	12.22	2.15	5.55
20	54.54	0.821	-5.17	20.55	7.73	0.134	12.97	2.27	5.89
30	56.62	0.929	-12.82	23.44	7.48	0.129	14.78	2.55	6.73

APPENDIX H - Shonkinite probe data from Tureck-Schwartz (1992)

	Salite-1	Salite-2	Plagioclase	Sanidine
SiO_2	53.14	50.35	54.15	61.75
Al_2O_3	1.17	3.13	32.12	21.02
TiO_2	0.34	0.70		
FeO*	5.50	6.68		
MnO		0.14		
MgO	14.86	14.75		
CaO	23.00	22.87	11.01	1.68
Na_2O	0.41	0.71	4.41	4.88
K_2O		0.07	0.50	7.90

Salite-1 = BP-S16 Tureck-Schwartz 1992
Salite-2 = SS-2 Nash 1970
Plagioclase = BP-S18a Tureck-Schwartz 1992
Sanidine BP-S39 = Tureck-Schwartz 1992

APPENDIX I - Incremental calculations for fractional crystallization from shonkinite

	SiO2	TiO2	MgO	Al2O3	FeO	MnO	CaO	K2O	Na2O
Average shonkinite composition	52.48	0.63	3.82	17.19	8.24	0.17	7.83	5.11	3.37
Average augite composition	51.75	0.52	14.81	2.15	6.09	0.14	22.94	0.07	0.56
Average sanidine composition	61.75			21.02			1.68	7.9	4.88
Augite									
% crystals removed									
0	52.48	0.630	3.82	17.19	8.24	0.170	7.83	5.11	3.37
2	52.49	0.632	3.60	17.50	8.28	0.171	7.52	5.21	3.43
4	52.51	0.635	3.36	17.82	8.33	0.171	7.20	5.32	3.49
6	52.53	0.637	3.12	18.15	8.38	0.172	6.87	5.43	3.55
8	52.54	0.640	2.86	18.50	8.43	0.173	6.52	5.55	3.61
10	52.56	0.642	2.60	18.86	8.48	0.173	6.15	5.67	3.68
15	52.61	0.649	1.88	19.84	8.62	0.175	5.16	6.00	3.87
20	52.66	0.658	1.07	20.95	8.78	0.178	4.05	6.37	4.07
30	52.79	0.677	-0.89	23.64	9.16	0.183	1.35	7.27	4.57
	52.48			17.19			7.83	5.11	3.37
Sanidine									
% crystals removed									
0	52.48	0.670	5.54	17.19	8.08	0.140	7.83	5.11	3.37
2	52.29	0.682	4.67	17.11	8.05	0.139	7.96	5.05	3.34
4	52.09	0.695	3.75	17.03	8.02	0.139	8.09	4.99	3.31
6	51.89	0.709	2.80	16.95	7.99	0.138	8.22	4.93	3.27
8	51.67	0.723	1.81	16.86	7.96	0.138	8.36	4.87	3.24
10	51.45	0.737	0.78	16.77	7.93	0.137	8.51	4.80	3.20
15	50.84	0.777	-2.02	16.52	7.83	0.136	8.92	4.62	3.10
20	50.16	0.821	-5.17	16.24	7.73	0.134	9.37	4.41	2.99
30	48.51	0.929	-12.82	15.55	7.48	0.129	10.47	3.91	2.72

Bailey, D.G., Warner, P.W., Kisner, K.L., and Everdell, J.W., 1994, Evidence for diffusive chemical exchange during mingling of basaltic and granitic magmas: a necessary precursor to magma mixing, *Geological Society of America Abstracts with Programs*, 26, no. 3, 4.

Beall, J.T., 1973, Mechanics of intrusion and petrochemical evolution of the Adel Mountain Volcanics: Ph.D. Thesis, University of Montana, 104 pp.

Caroff, M., 1995, Open system crystallization and mixing in two-layer magma chambers: *Lithos.*, 36, 85-102.

Caroff, M., 1993, Trace element behavior in the alkali basalt-comenditic trachyteseries from Mururoa Atoll, French Polynesia: *Lithos.*, 30, 1-22.

Cunningham, W.L., 1995, Petrogenesis of the Corea Pluton, coastal Maine magmatic province, unpublished B.A. thesis from Amherst College, Amherst, MA, 47 pp.

Deer, W.A., Howie, R.A., and Zussman, J., 1963, Rock Forming Minerals. William Clowes and Sons: London, vol. 1, 2, 4.

Delany, P.T., Gartner, A.E., 1997, Physical processes of shallow mafic dike emplacement near the San Rafael Swell, Utah, *Geology*, 25, 9, 1177-1193.

DePaolo, D.J., 1981, Trace element and isotopic effects of combined wallrock assimilation and fractional crystallization, *Earth and Planetary Science Letters*, 53, 189-202.

Edmund, C.A., 1980, Magma immiscibility in the Shonkin Sag laccolith, Highwood Mountains, central Montana: M.S. Thesis, University of Montana, 98 pp.

Foster, D.A., and Hyndman, D.W., 1990, Magma mixing and mingling between synplutonic mafic dikes and granite in the Idaho-Bitterroot batholith, *Geological Society of America Memoir*, 174, 347-357.

Frost, T.P. and Mahood, G.A., 1987, Field, chemical, and physical constraints on mafic-felsic magma interaction in the Lamarck Granodiorite, Sierra Nevada, CA, *Geological Society of America Bulletin*, 99, 272-291.

Harlan, S.S., 1991, New Ar/Ar isotopic dates from the AMV: Implications for the relationship between deformation and magmatism in the Montana disturbed belt *Geological Society of America Abstracts with Programs*, 23, 136.

Hearn, B.C., Collerson, K.D., Upton, B.G.J. and Macdonald, R.A., 1991, Ancient and enriched upper mantle beneath north-central Montana:Evidence form xenoliths, *in* Montana Bureau of Mines and Geology, Special Publication, 100, 133-135.

Hearn, B.C., 1989, Introduction in Montana High-Potassium Igneous Province Field Trip Guidebook T346: *American Geophysical Union*, 1-5.

Hyndman, D.W., Alt, D., and Sears, J.W., 1988, Post-archean metamorphic and tectonic evolution of western MT and northern ID p. 333-361, *in* Metamorphism and Crustal Evolution of the Western United States, ed. Ernest, W.G.: Prentice Hall, NJ, 1142.

Hyndman, D.W., Tureck-Schwartz, K., and Foland, K., 1988, Chemical and isotopic evidence for mafic potassic magmas from an old K-enriched mantle source and for Eocene crustal melting in the central Montana alkalic provincce: *Geological Society of America Abstracts with Programs*, 20, A195.

Hyndman, D.W., 1985, Source and formation of the Idaho Batholith: *Geological Society of America Abstract with Programs*, 17, no. 4, 226.

Hyndman, D.W., 1985, Petrology of Igneous and Metamorphic Rocks Second Edition. McGraw-Hill Inc: N.Y., 786 pp.

Irving, A.J. and OÕBrien, H.E.,1991, Isotopic and trace-element characteristics of late Cretaceous to Oligiocene mafic volcanics from west-cental Montana: Implications for Tertiary tectonics and magma genesis, *in* Central Montana Alkalic Province Guidebook, Special Publication, 100, 140-142.

Johnson, D.M., Hooper, P.R., and Conrey, R.M., XRF analysis of rocks and minerals for major and trace elements on a single low dilution Li-tetraborate fused bead, *Advances in X-Ray Analysis*, 41, in press.

Kuhn, P.W., 1983, Magma immisicibility in the Box Elder laccolith of north-central Montana: M.S. Thesis, University of Montana, 86 pp.

Lindline, J., Crawford, W.A., Crawford, M.L., 1993, Magma mixing and mingling on Deer, Niblack, and Etolin islands, southeastern Alaska, *Geological Society of America Abstracts with Programs*, 25, no. 2, 34.

Lyons, J.B., 1944,Geology of the northern Big Belt Range, MT: *Geological Society of America Bull.*, 55, 445.

McBirney, A.R, 1993, Igneous Petrology. Jones and Bartlett Publishers: Boston, MA, 508 pp.

McCallum, S., O'Brien, H., and Irving, A., 1989, Geology of the Highwood Mountains, Montana: A survey of magma types and sources, *in* Montana High-Potassium Igneous Province Field Trip Guidebook T346: *American Geophysical Union*, 23-35.

Nash, W.P and Wilkinson, J.F.G., 1970, Shonkin Sag Laccolith, Montana, Part I. Mafic minerals and estimates of temperature, pressure, oxygen fugacity, and silica activity, *Contr. Mineral. Petrol.*, 25, 241-269.

O'Brien, H.E., Irving, A.J., and McCallum, I.S., 1988, Complex zoning and resorption of phenocrysts in mixed potassic magmas of the Highwood Mountains, MT: *Am. Mineralogist*, 73, no. 9, 1007-1024.

Raymond, Loren A., 1995, Igneous Petrology. Wm. C. Brown Publishers: Boston, MA, 240-249.

Rutland, Carolyn, 1985, Geochemistry of the Elkhorn Mountain volcanics, southwestern Montana: Implications for the early evolution of a volcanic-plutonic complex, Michigan State University, Ph.D. thesis, 96 pp.

Russell, J.K., and Halleran, A.D., 1989, Trace elements formulated as Pearce Elelment Ratios (PER) I: Insights into magmatic differentiation, p. 55-72, *in* Theory and Application of Pearce Element Ratios to Geochemical Data Analysis, ed. Russell, J.K., and Stanley, C.R.: Geological Association of Canada, Vancouver, British Columbia, 315 pp.

Sabine, P.A., 1989, Setting standards in petrology: The commission on systematics in petrology, *Episodes*, 12, 2, 84-86.

Schmidt, R., 1977, Geologic map of the Craig quadrangle, Lewis and Clark and Cascade Counties, MT, USGS, GQ-1411, scale 1:24,000.

Sheriff, S., and Gunderson, J., 1990, Age of the Adel Mountain Volcanic field, west-central Montana: *Isochron/West*, 56, 21.

Sorensen, H., 1986, The Alkaline Rocks - A review: *Fortschr. Miner.*, 64, 63-86.

Sparks, R., and Sigurdsson, H., 1977, Magma mixing: a mechanism for triggering acid explosive eruptions, *Nature*, 267, 315-318.

Swenson, Robert F., 1988, Adel Mountain volcanics: A trip through geo-fantasyland, B.A. Thesis, University of Montana, 45 pp.

Tilling, R.I., 1973, Boulder Batholith, Montana: A product of two contemporaneous but chemically distinct magma series, *Geological Society of America Bulletin*, 84, 3879-3900.

Tureck-Schwartz, K., and Hyndman, D., 1991, High-potassium igneous rocks of the Bearpaw Mountains, north-central Montana: p. 110-120 *in* Guidebook of the Central Montana Alkalic Province, D.W. Baker and R.B. Berg, editors, Montana Bur. Mines and Geol Spec.Publ, 100, 201 pp.

Tureck-Schwartz, K., 1992, The association of alkalic and subalkalic rocks in the Bearpaw mountains, M.S. Thesis, University of Montana, 160 pp.

Watson, E.B., 1976, Two-liquid partition coefficients: Experimental data and geochemical implications, *Contrib. Mineral. Petrol.*, 56, 119-134.

Whiting, C.K., 1977, Small laccoliths and feeder dikes of the northern Adel Mountain Volcanics: M.S. Thesis, University of Montana, 74 pp.

Wilson, M., 1994, Igneous Petrogenesis - A Global Tectonic Approach. Chapman and Hall: London, England, 466 pp.